University of Tartu
Faculty of Science and Technology
Institute of Ecology and Earth Sciences
Department of Geology

Kaarel Mänd

Geochemistry, microstructure and origin of recent phosphorites on the Namibian margin

Master's thesis in geology

Supervisors: Kalle Kirsimäe
Aivo Lepland
Jake Bailey

Tartu 2016

Geochemistry, microstructure and origin of recent phosphorites on the Namibian margin

Phosphorites are crucial components of the global phosphorous cycle and a major source of fertilizers. Their formation is poorly understood, but the role of microbes has been strongly suggested. To determine microbial influence, in this thesis the nucleation and primary growth of phosphate minerals in natural phosphorites was studied using XRD, ICP-MS and SEM analyses. From recent phosphorite sediments on the Namibian shelf authigenic phosphate pellets were extracted. The pellets contain conspicuous phosphatic microrods, which co-occur with film-like organic substances. The structures superficially resemble phosphatized microbes, but there are frequent cases of the rods intersecting each other. Furthermore, there exists a continuum of forms from rods to dumbbells to spherical aggregates. A very similar succession of phosphate microstructures, fluoroapatite-gelatine nanocomposites, have previously been reported from abiological laboratory experiments. The microstructures do not represent microbial casts, but abiological precipitates, which urges caution when interpreting similar structures in other phosphorites. The bacterially produced organic film possibly acts as the major nucleation template for phosphate minerals and thus supports the role of microbes in the formation of phosphorites.

Phosphogenesis, apatite nucleation. P420 Petrology, mineralogy, geochemistry

Retsentsete Namiibia šelfimere fosforiitide geokeemia, mikrostruktuur ja päritolu

Fosforiidid on olulised komponendid maailma fosforiringes ja kriitilise tähtsusega ressursid väetiste tootmisel. Nende tekkemehhanismi mõistetakse veel halvasti, aga hiljutised uuringud on rõhutanud mikroobide olulist rolli nende moodustumisel. Mikroobse mõju selgitamiseks uuriti käesolevas töös fosfaadi nukleerumist ja esmast kasvu Namiibia šelfimere tänapäevastes fosforiidisetetes. Autigeenne fosforiit esineb nendes setendites fosfaatsete teradena millede kohati poorses sisestruktuuris leidub orgaanilise matriitsiga seotult hulgaliselt fosfaatseid mikropulgakesi. Visuaalselt meenutavad need moodustised fosfatiseerunud mikroobe, aga erinevalt mikroobsetest struktuuridest on täheldatavad osakeste lõikumine ja läbikasvulised agregaatmoodustised. Samuti moodustavad pulgakesed morfoloogiliselt pideva üleminekulise rea pulkadest hantlikujulisteks ja sfäärilisteks vormideks. Sarnast morfoloogilist arengurida on täheldatud ka fosfaadi setitamise laborieksperimentides, nn. fluoroapatiidi-gelatiini nanokomposiitide puhul. Uuritud fosfaatsed pulgakesed on seega abioloogilised, mitte mikroobsed fossiilid ja seetõttu tuleks sarnaste struktuuride tõlgendamisega edaspidi ettevaatlik olla. Struktuuridega seotud orgaaniline substants on tõenäoliselt bakteriaalse metabolismi kõrvalprodukt ning mängib suurt rolli apatiidi nukleerumisel, mis viitab mikroobide suurele rollile fosforiitide tekke esmaetappidel.

Fosfogenees, apatiidi nukleerumine. P420 Petroloogia, mineroloogia, geokeemia.

Table of Contents

Introduction

Phosphorous, an essential energy carrier and building block of life, is the primary limiting nutrient of marine biological productivity in a geological time scale (Tyrrell, 1999). Consequently, the phosphorus cycle is intimately coupled to the cycles of carbon and other biologically significant elements, having a substantial influence on atmospheric levels of oxygen and carbon dioxide as well as on the history of life (e.g. Cárdenas and Harries, 2010; Martin, 1996; Papineau, 2010; Papineau et al., 2013; Planavsky et al., 2010; Pufahl and Hiatt, 2012). Phosphorites – rocks that contain >9% of P_2O_5 (Filippelli, 2011) – constitute a central part of the phosphorous cycle, being its most important long-term sink (Delaney, 1998). Phosphorites are also a critical non-renewable resource for agriculture, used for producing phosphatic fertilizer (Cordell et al., 2009), and the worldwide drive towards a more sustainable P management is wholly dependent on a comprehensive understanding of its cycling (Crosby and Bailey, 2012).

Despite their great scientific and economic importance, the origins of phosphorites are to a large degree still uncertain. The necessary processes forming phosphorites involve the whole marine P cycle starting from P weathering and release on continents, transport to oceans, incorporation/take up into biomass, accumulation/deposition with organic-rich sediments, release from decaying organic matter and pre-concentration, and finally, precipitation of a stable Ca-phosphate phase – apatite (Filippelli, 2011; Föllmi, 1996; Ruttenberg, 2014).

Much of scientific understanding of the formation of phosphorites and of the P cycle itself has undergone a significant revision over the past decades (Filippelli, 2011). Long-standing debates involve, for example, the relative importance of Fe/Mn hydroxides and organic matter in the flux of P towards sediments; the nature of processes which remobilize this deposited P in sediments; the spatial and temporal distribution of P burial episodes and the reasons for such episodic-temporal distribution of phosphorites. Perhaps the least well-known are the processes and substrates that are involved in the transition from pore water P enrichment to the beginning of the precipitation of apatite minerals – essentially the very first stages of phosphogenesis (Crosby and Bailey, 2012), which is what this thesis is specifically interested in.

Recent studies have highlighted the role of microbial processes mediating phosphorous-cycling by creating sinks for marine phosphorous and eventually phosphorite formation (Arning et al., 2009, 2008; Brock and Schulz-Vogt, 2011; Goldhammer et al., 2010; Schulz, 1999; Schulz and Schulz, 2005). It is of utmost importance that these studies have revealed in marine sediments several genera of sulfur-oxidizing bacteria that are capable of storing intracellular polyphosphate reserves (e.g. *Beggiatoa, Thiomargarita*). These microorganisms act like peculiar "phosphate pumps" capable storing intracellularly polyphosphate under oxic conditions, then hydrolyzing the polyphosphate and releasing phosphate under anoxic conditions (Brock and Schulz-Vogt, 2011; Schulz and Schulz, 2005). This means, that the bacterial phosphate "pumping" can lead to supersaturation of the pore water with respect to apatite and eventually its precipitation (Arning et al., 2009; Goldhammer et al., 2010). However, the mechanisms how apatite becomes precipitated and/or if and to what extent the precipitation itself, apart from creating P-supersaturation, is bacterially mediated or influenced in such processes, are unknown.

In modern oceans a major sink of phosphorous and the formation of phosphorites occurs at the continental margins influenced by upwelling ocean currents which carry P-rich deep ocean water that stimulates primary production in surface water leading, thus, to accumulation of organic-rich sediments and organically bound phosphorous. Such hot-spots of modern phosphorite deposition are the Namibian and the Peruvian shelves (Föllmi, 1996). The phosphorites of the Namibian and southern to eastern South African shelves are known for more than 100 years, and their formation and economic potential has attracted attention since then (Coles et al., 2002). Phosphorite formation at the Namibian shelf is a complex phenomenon involving changes in sea level that has resulted in the reworking, transport and concentration of earlier phosphorites (Compton and Bergh, 2016), and presumably microbially influenced (direct) phosphate precipitation (Schulz and Schulz, 2005). It was on the Namibian shelf where giant sulfur-oxidizing bacteria possibly controlling the phosphogenesis in these sediments were first discovered (Schulz, 1999).

The central question motivating this study is whether or not phosphate precipitation is controlled or influenced by microbial/biological structures. I focus on studying the micro- and nanofabric of modern phosphorites from the shelf sediments off the coast of Namibia. The overall goal is to determine any present and preserved microbial structures and their relation to the overall fabric of phosphorites in Namibian shelf.

P-cycle and phosphogenesis

The whole marine P cycle is very complex and constitutes several steps (Filippelli, 2011; Föllmi, 1996; Ruttenberg, 2014):

(1) P is weathered from rocks on the continents and is carried to the oceans mainly via riverine transport, and to a lesser degree by wind, in various forms, like dissolved inorganic or organic P, included in particulate organic matter, absorbed onto Fe-mineral particles or as detrital phosphate minerals (Compton et al., 2000);

(2) Having reached the ocean, most of the P is dispersed within sediments, while roughly 30% of it, called the reactive phosphorous phase, becomes rapidly incorporated in planktonic biomass. As a consequence of this, photic zone phosphate concentration in seawater is generally very low (Compton et al., 2000; Filippelli, 2011);

(3) P is carried from the photic zone towards the sediment via sorption or incorporation onto/into particulate forms, such as dead organic matter, biominerals, continentally or hydrothermally derived Fe/Mn-oxide particles, or oxide coatings on mineral surfaces, of which particulate organic matter makes up the majority (Delaney, 1998; Krajewski et al., 1994). As far as the delivery of reactive P to the sea floor far exceeds that delivered into oceans from continental weathering, the vast majority of P is not incorporated into sediments, but is rather regenerated into dissolved form once it has reached the sea floor (Delaney, 1998; Föllmi, 1996). However, in almost every marine environment, a fraction is still incorporated in the sediment – estimated to be roughly 5% of the delivered P (Föllmi, 1996).

(4) Several processes contribute to the release of dissolved phosphate form all of these phases during sinking or during early diagenesis in the topmost sediments, meaning that phosphate concentrations in bottom water and in sediment pore water are substantially higher than in surface waters (Filippelli, 2011; Krajewski et al., 1994);

(5) In the majority of the world's ocean bottom environments the P concentrations are high enough to allow for the precipitation of authigenic phosphate phases – a process known as phosphogenesis – though the concentration can be largely varying depending on the ratio between terrigenous input and sinking organic matter flux (Ruttenberg and Berner, 1993; Delaney, 1998). Areas of low terrigenous input and high biomass production can show a substantially higher concentration of authigenic phosphatic matter, but typically these

concentrations are still not enough to be classified as phosphorites (Filippelli, 2011; Ruttenberg, 2014);

(6) The final step in the transformation of P-rich sediments into true phosphorites involves multi-stage sedimentological processes, such as winnowing and reworking, driven either by current activity or sea-level changes (Baturin, 1971; Filippelli, 2011; Föllmi, 1996). Episodes of these sedimentological processes can alternate with phosphate precipitation in what are known as “Baturin cycles” (Föllmi, 1996).

The most common phosphate mineral is the Ca-containing apatite, but due to the high tolerance of apatite minerals for elemental and molecular substitutions, it is more properly referred to as a large family of minerals (Omelon et al., 2013). Authigenic apatite is commonly precipitated as carbonate fluoroapatite (CFA), which during diagenesis starts to lose carbonate and transforms into fluoride-rich CFA or francolite that is the most common form of apatite in ancient phosphorites (Jarvis et al., 1994; Ruttenberg, 2014).

Apatite precipitation in the natural environment depends on several physical/chemical parameters like pH, temperature and redox potential, but there is no consensus on the specific mechanisms (Ruttenberg, 2014). Much less ambiguous is the effect of supersaturation. At a lower supersaturation state, apatite can nucleate only in a heterogeneous manner, e.g. making use of a compatible nucleation surface, while at higher values, homogeneous or spontaneous nucleation becomes possible. Still, as a general rule, homogeneous nucleation is kinetically less favored due to a significantly higher activation energy, meaning that nucleation on a preexisting surface is more common in nature (Omelon et al., 2013). Direct apatite precipitation from solution is, however, a very slow process due to its high interfacial free energy, which makes its role in producing phosphorite deposits of an economic value questionable (Ruttenberg and Berner, 1993). At very high concentrations ($\sum PO^4$ = 400–600 μM), a much more effective pathway becomes kinetically possible. It involves the precipitation of different metastable Ca-phosphate phases, such as struvite, octacalcium phosphate or amorphous calcium(-magnesium) phosphate as precursor phases, which later serve as a template for apatite formation or convert directly into it (Krajewski et al., 1994; van Cappellen and Berner, 1991). Geochemical signals of such transformations have been previously found in modern phosphorites, such as those off the coast of Peru (Froelich et al., 1988; Krajewski et al., 1994).

High supersaturations are also deemed necessary for the rapid nucleation events that could produce the high concentrations of stable nuclei in many recent and ancient phosphorites – for example Lamboy (1990a) estimated the nucleation density (number of individual apatite particles) in modern phosphorites to be as high as 10^9 cm^{-3}. Local nucleation events would additionally explain the occurrence of modern phosphorites as discrete crusts, nodules or pellets (Föllmi, 1996; Krajewski et al., 1994).

The concentration of dissolved P in modern bottom seawater is on average between 1.5 and 2.5 μM (Filippelli, 2011; Omelon et al., 2013). Nucleation of apatite from such a solution is expected and observed taking place in a wide variety of marine environments (Föllmi, 1996). Diffuse phosphate phases appear in-deep ocean sediments and have been implicated as a major sink in the P cycle, when taking account the geographical extent of such environments (Delaney, 1998; Filippelli and Delaney, 1996). Estuaries and continental margins have a significantly higher iron and organic matter flux (Krajewski et al., 1994) and the shallower water column leaves fewer opportunities for phosphate-associated particulate matter to be degraded (Krajewski et al., 1994). These factors are responsible for a much higher phosphate concentration and, thus, more intense P burial (Delaney, 1998; Reimers et al., 1996; Ruttenberg and Berner, 1993). Nevertheless, in both environments, authigenic phosphate is too scattered and its formation process is too slow to produce economic deposits (Föllmi, 1996).

The main areas of importance in phosphorite formation are the major upwelling systems on continental margins. This is due to their outsized role in biomass production and thus in the flux of sinking organic matter to the sediments. Indeed, the great majority of modern phosphorites are forming in regions of upwelling (Föllmi, 1996), such as on the Namibian (Baturin, 2000; Baturin and Bezrukov, 1979; Compton and Bergh, 2016; Summerhayes et al., 1973), Chilean and Peruvian (Burnett, 1977; Burnett et al., 2000; Veeh et al., 1973), Mexican (Jahnke et al., 1983; Schuffert et al., 1998), and East Australian (O'Brien and Heggie, 1988; O'Brien and Veeh, 1980) shelves and in the Arabian Sea (Schenau et al., 2000). In these environments, P supersaturation of a high degree have been shown to occur in the topmost cm-s of sediment pore water. Due to the high flux of easily degradable organic matter, the oxygen levels in the overlying bottom waters are very low, which means that the redoxcline – the interface between oxic and anoxic environments – lies very close to the sediment-water interface, and all redox-dependent reactions of phosphate release must take place in a very

shallow zone (Froelich et al., 1988; Goldhammer et al., 2010; Holmkvist et al., 2010; Schulz and Schulz, 2005). Though the phosphate content in those pore waters is generally still lower than what is needed for the formation of apatite precursors, sufficient concentrations might be achieved periodically. The quick precipitation of these phases might also lead to the rapid depletion of porewater phosphate and could explain why higher values are rare (Krajewski et al., 1994). More interestingly, even when below the level needed for the precipitation of precursors, the recorded concentrations of dissolved phosphate in some of these environments cannot be explained simply by decomposition of sedimentary organic matter (Froelich et al., 1988; Krajewski et al., 1994). This has led many to turn towards more explicitly biogenic solutions to the problem of the intensive phosphogenesis needed for the production of phosphorites.

Microbial influences on phosphorite formation

Microbially mediated reactions have been shown to be involved in most steps of the formation of phosphorites (Crosby and Bailey, 2012). Chemical weathering of P-bearing rocks, which produces most of the reactive P flux into oceans, is carried out with the help of microbial processes (Compton et al., 2000). Microbes have also long been known to play an integral part in regulating the rate at which dissolved phosphate is released from reactive sedimentary P reservoirs to pore waters (Föllmi, 1996; Krajewski et al., 1994). Different heterotrophic microbial mechanisms are involved in the degradation of particulate organic matter in the sediments (Arning et al., 2009). P-binding Fe/Mn phases are dissolved once exposed to the kind of reduced conditions that allow for bacterial dissimilatory iron reduction (Ruttenberg and Berner, 1993). Aerobic microbes also play a role in the dissolution of phosphatic skeletal remains (Smith et al., 1977).

In the late 1980s and 1990s, however, researchers began to speculate on the importance to phosphogenesis of those sediment microbial communities, which have the ability to uptake and release phosphate depending on the prevailing redox state and thus significantly influence the geochemical potential of their environment (Föllmi, 1996; Gächter et al., 1988; Krajewski et al., 1994). It was suspected that one such type of microbes might be the colorless filamentous sulfur bacteria that commonly form mats in areas of phosphogenesis (Bailey et al., 2013; Krajewski et al., 1994).

A significant boost to this line of thinking was given in 1999 when the largest known bacteria, the coccoid sulfur-oxidizing chemoheterotroph *Thiomargarita namibiensis* were discovered and characterized (Schulz, 1999). These bacteria inhabit the sulfide-rich redoxcline of modern oxygen-poor oceanic shelf sediments in a variety of locations around the world, but the most well-known locality is off the coast of Namibia (Bailey et al., 2011; de Beer et al., 2006; Girnth et al., 2011; Kalanetra et al., 2005; Salman et al., 2013; Schulz and Schulz, 2005). The common metabolic pathway of these bacteria involves the oxidation of reduced sulfur species using dissolved oxygen or nitrate, which they store in a giant central vacuole. All of these substances are abundant in significant concentration in their environment, but at different times, that is due to the seasonally shifting redox conditions on the Namibian shelf (Monteiro et al., 2006). Due to the unstable nature of the environment they inhabit, however, *Thiomargarita* also utilize a complementary metabolic track, in which they scavenge dissolved phosphate released from decaying organic matter that they store in the form of intracellular granules of polyphosphate, an energy and P storage compound. In anaerobic, sulfidic conditions, this compound is used up and the resultant phosphate is released into the surrounding environment in a short pulse (Brock and Schulz-Vogt, 2011; Schulz and Schulz, 2005). In addition to *Thiomargarita*, the polyphosphate storage is important in the metabolically similar *Beggiatoa* and *Thioploca* (Holmkvist et al., 2010; Jørgensen and Gallardo, 1999) and also in iron-oxidizing bacteria that tend to inhabit similar hypoxic conditions (Singer et al., 2011), but also in a variety of other groups in similar environments (Jones et al., 2016).

This mechanism of microbial phosphate cycling is strongly implicated as responsible for producing the conditions required for phosphogenesis in modern sediments. Evidence for this is provided by the intimate spatial correlation between the abundance of sulfide-oxidizers and phosphate concentration both in pore water and in solid phase (Arning et al., 2009, 2008; Schulz and Schulz, 2005) along with experimental proof of phosphate release by these microbes in response to sulfidic conditions (Brock and Schulz-Vogt, 2011), and isotope studies indicating the rapid precipitation as apatite of microbially-released phosphate (Goldhammer et al., 2010). Though some studies have cast doubt on the uniqueness of this process in being able to produce significant dissolved phosphate concentrations (Arning et al., 2009; Holmkvist et al., 2010), polyphosphate metabolism has been proposed as the

mechanism responsible for the creation of many ancient phosphorites (Alsenz et al., 2015; Arning et al., 2009; Bailey et al., 2013, 2007; Crosby et al., 2014; Crosby and Bailey, 2012).

Microbes have even been implicated in influencing the temporal distribution of phosphorites throughout geological time. This distribution is characterized by the episodic occurrence of widespread phosphorites, such as in the Palaeoproterozoic, Neoproterozoic to Cambrian, Permian, Cretaceous to Eocene, and Miocene, separated by long periods of relative paucity (Cook and Shergold, 1984; Filippelli, 2011; Lepland et al., 2013b; Ruttenberg, 2014). Some authors emphasize the key role of sedimentary processes and assert that the distribution of phosphorites in discrete intervals of geological time is a coincidental result of prevailing sedimentary conditions favoring the preservation of phosphorites during those periods (Filippelli, 2011). Others explain it through fluctuations in the riverine flux of continentally-derived phosphate into the sea, which is in turn related to changes in weathering conditions (Föllmi, 1996; Papineau, 2010; Planavsky et al., 2010). However, recent papers have put forward a new explanation for the first appearance of phosphorites roughly 2.0 Ga ago, shortly after the Great Oxygenation Event (Lyons et al., 2014; Pufahl and Hiatt, 2012). According to this scenario, the leap in sulfide mineral weathering caused by the onset of oxic conditions lead to the buildup of the marine sulfate pool. Together with the establishment of sediment redox boundaries, it allowed for the evolution of modern sulfur-cycling bacterial communities and the associated polyphosphate metabolism. With the establishment of the required geobiochemical conditions for phosphogenesis, the formation of the first phosphorites became a possibility (Crosby and Bailey, 2012; Lepland et al., 2013b).

Geological setting

The phosphorites of the Namibian and eastern/southern South African shelves were discovered in the end of the 19th century (Murray and Renard, 1891). In the 1970s, the Namibian shelf, along with the Peru/Chilean shelf, was one of the first places in the world where modern formation of phosphorite was observed (Summerhayes et al., 1973). Scientific and economic interest resulted in an extensive study of the geology of the deposit, especially from the 70s to early 90s, results of which are summarized in (Rogers and Bremner, 1991). During the past few years, world phosphate price fluctuations and a more immediate understanding of the critical nature of this resource has reignited commercial interest in the mining of Namibian phosphorite (Coles et al., 2002). This has resulted in an intensive commercial study campaign, the results of which were very recently summarized by Compton and Bergh (2016).

The Namibian shelf, which formed ca. 400 Ma ago during the breakup of Gondwana, is known for its unusual broadness and deepness, extending to 400 m water depth. It is generally divided into three zones: the inner shelf, up to 130 m depth; the middle shelf, up to 300 m; and the outer shelf, up to 400-500 m. The basement rocks are Proterozoic up to the middle shelf and Cretaceous to Cenozoic in the outer shelf. These are covered by a thin, poorly documented Cenozoic succession, terminated by an erosional surface, on which late Cenozoic to modern sediments lie. The main sources of terrigenous input onto the shelf are the Kunene and Orange rivers, marking the northern and southern boundaries of Namibia; and windblown dust from the Namib Desert (Compton and Bergh, 2016; Eckardt and Kuring, 2005). The nearshore facies is heavily influenced by storms and consists of sand and gravel. On the inner shelf, it is replaced by a 15 m thick layer of Pleistocene to recent diatomaceous mud (Baturin, 2000), the composition of which is influenced by the sediment flux carried by the Kunene river in the north, but grades into an organic-rich diatomaceous ooze towards the south. The middle and outer shelves are dominated by terrigenous sediments off the Kunene river delta in the north and carbonate-rich shelly or nannofossil sediment elsewhere. The Pliocene to recent succession on the shelf is highly condensed but is represented by 600 m thick sediment pile on the upper slope (Compton and Bergh, 2016).

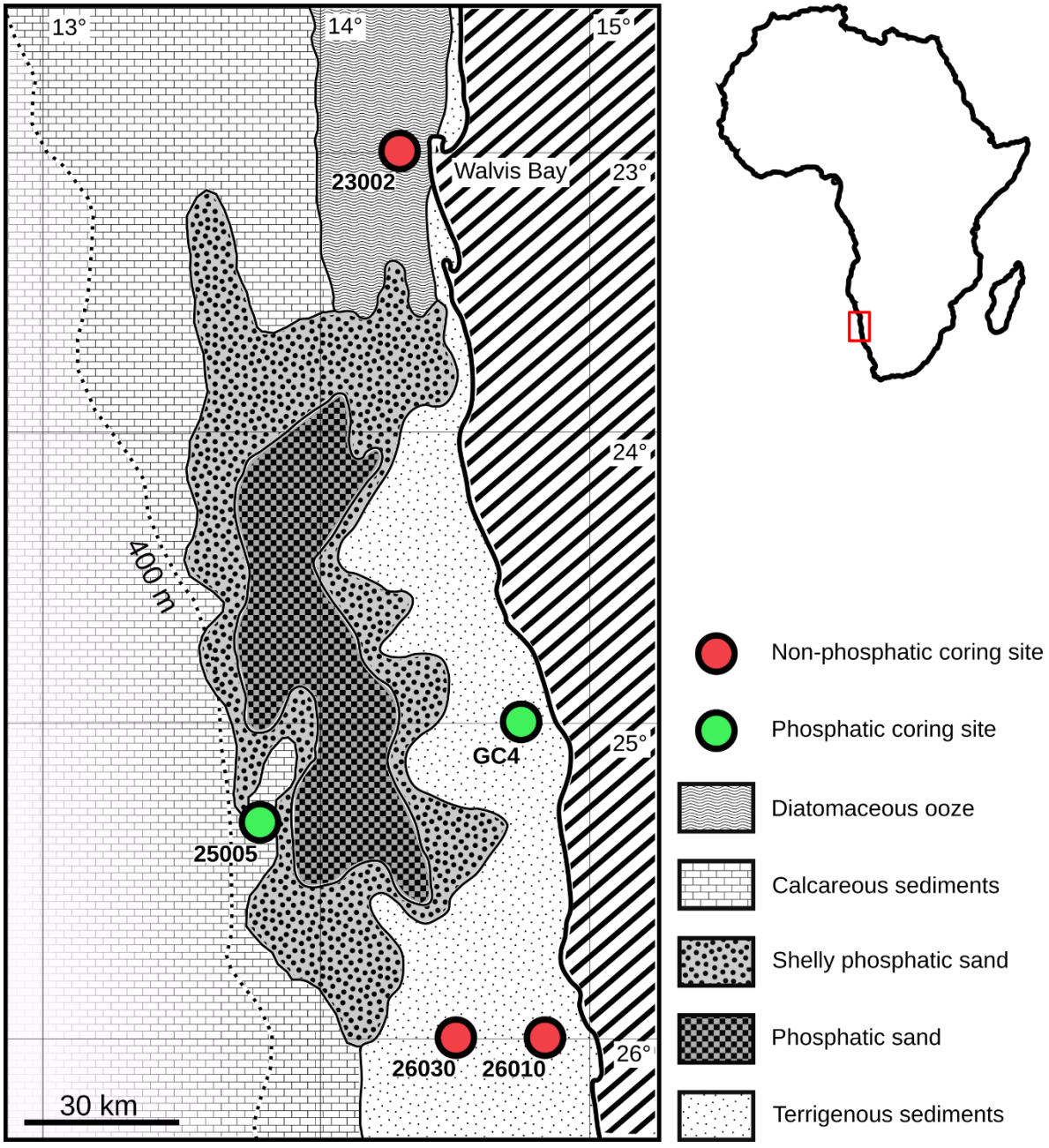

Figure 1: Sediment type distribution on the southern part of the Namibian shelf along with coring sites. Modified after (Baturin, 2000).

The entire southwestern African shelf and especially its Namibian section is dominated by some of the strongest upwelling in the world, the Benguela Upwelling System. The rising nutrient-rich deep ocean waters fuel the world's most productive eastern boundary marine ecosystem (Carr, 2001), which is associated with intense organic carbon burial (Inthorn et al., 2006). This flux of sinking organic matter is the main factor enabling the formation of

phosphorites on the inner shelf. Phosphorite deposits of the sea floor, ranging in age from late Oligocene to modern extend from the southern shelf of South Africa up to the Kunene River (Baturin, 2000; Compton et al., 2004, 2002; Compton and Bergh, 2016). This phosphorite usually occurs in the form of francolite pellets, which are roughly a few hundred micrometers in diameter, along with concretionary authigenic forms, phosphatized mollusk molds and very occasionally recent phosphatic brachiopods (Baturin, 2000). Skeletal fragments are also ubiquitous, but make up no more than 10-20% of the total phosphorite. Apatite in these sediments is also commonly associated with glauconite sand and microscopic pyrite (Compton and Bergh, 2016).

Based on its genesis, Namibian phosphorites can broadly be divided into two classes: modern phosphatic sediments forming in the diatomaceous ooze of the inner shelf, and reworked, more extensive phosphorite of the middle to outer shelf (Baturin, 2000). The area where diatomaceous ooze is distributed is known from the vicinity of Walvis Bay and is situated between 50 and 140 m of depth. The phosphatic component in the diatomaceous mud is modest, but is prevalent in the sand fraction (Baturin, 2000). It is characterized by phosphatic concretions and pellets, which range from fragile and light-colored non-lithified aggregates to hard, dark and lithified pellets. Additionally, these sediments contain abundant fish fragments and coprolites. This phosphorite is known to be late Pleistocene to Holocene in age and is considered to be authigenic (Baturin, 2000; Veeh et al., 1974).

The economically-important phosphorite deposit of the middle to outer shelf between Walvis Bay and Lüderitz is located at between 180 to 500 m depth and is genetically and morphologically distinct from the modern phosphorites of the inner shelf. The focus of the recent study campaign was on this deposit, which is described in detail by Compton and Bergh (2016). The deposit consists of a 1-2 m thick P-rich layer, which displays a coarsening upward succession from muddy to increasingly more sandy and gravelly. Aside from phosphorite sand, skeletal fish debris, foraminal and bivalve shells and some terrigenous component can be recovered. As a whole, strontium isotope stratigraphy places the formation time of this phosphorite from the late Miocene to Pleistocene, beginning at roughly 5.8 Ma, with the majority of it forming during the Pliocene and Pleistocene. Higher resolution Sr isotope measurements combined with biostratigraphy show an upward trend towards younger ages, with the topmost layer late Pleistocene to early Holocene in age. However, there does remain the possibility of contamination of the Sr system (Compton and Bergh, 2016). Some

pellets show evidence of zonation consistent with multiple episodes of phosphorite formation; this, in addition to the sedimentary fabric and different strontium isotope ages for pellets in the same sample points to complex sedimentary reworking. Compton and Bergh (2016) explain the formation of this deposit through changes in sea level that has resulted in the reworking, transport and concentration of previously-formed authigenic phosphorite from the diatomaceous mudbelt to sediments further offshore, similar to what has previously been reported for South African deposits (Compton et al., 2004, 2002; Wigley and Compton, 2006). Authigenic phosphorite formation is interpreted to have taken place during sea level highstands and reworking during lowstands, beginning with the onset of glacial cycles in the Pleistocene (Compton and Bergh, 2016).

Materials and methods

The sediment samples used for this study were collected during oceanographic cruises on the research vessel Mirabilis in the central-southern shelf sea off the coast of Namibia. This was carried out as part of the doctoral school „RGNO – African Discovery Camp for Research-based Training" in April of 2014 and May of 2015. The 2014 material was unconsolidated phosphorite sand taken as a bulk sample using a van Veen grab, while in 2015, an Ocean Instruments, Inc. MC-400 multi-corer was used to sample a variety of unconsolidated sediments. A total of five cores were retrieved from a variety of locations on the shelf (Figure 1; Table 1). The top 10 cm of the cores were sectioned and sampled at 1 cm intervals; below that, the intervals were 2 cm in length. The samples were subsequently dried in the Sam Nujoma Campus of the University of Namibia, using a freeze-drier.

Table 1: Sediment cores.

ID	Latitude	Longitude	Water Depth (m)	Core length (cm)	Number of samples
23002	-23.00	14.37	40	25	18
25005	-25.00	14.74	47	25	18
GC4	-25.34	13.78	301	21	16
26030	-26.00	14.40	198	13	12
26010	-26.00	13.77	116	19	19

The mineralogical composition of whole rock samples was studied by means of X-ray diffractometry (XRD). Samples were pulverized by hand with an agate pestle and mortar and unoriented preparations were made. Preparations were scanned on Bruker D8 Advance diffractometer using Cu*K*α radiation and LynxEye positive sensitive detector in 2–70° 2Θ range. The quantitative mineralogical composition of the samples was interpreted and modelled by using the Rietveld algorithm-based program Topaz.

To determine phosphorite rare earth element (REE) composition and to study its microstructure, several apatite pellets were visually handpicked and extracted from bulk samples within apatite-containing cores. While apatite is a heavy mineral and should be able

to be extracted from lighter minerals via heavy liquid fractionation, the impurity and high porosity of the apatitic pellets made this method unfeasible.

The preparation of the pellets was done in three different ways. Some were cleaned in an ultrasound bath and placed on an adhesive carbon film. Others were placed on the adhesive carbon film, then cut with a scalpel to reveal their inner structure. A different set of pellets was embedded in epoxy, then finely ground down to reveal a cross-section. These were subsequently milled with a Leica EMRES101 Argon Ion Mill to produce a smooth and flat microsurface.

The embedded and polished pellets were used to determine the phosphorite REE composition. The REE in apatite were measured at the Department of Geology, University of Tartu, by laser ablation inductively coupled plasma mass spectrometry (LA-ICP-MS). In total, 61 spots were analysed from polished slabs. Measurements were made using an Agilent 8800 quadrupole ICP-MS coupled to a Cetac 213 nm HelEx fast-washout two-volume large-format cell using 25 µm spot size, at 5 Hz and ~2.5 j/cm^2 fluence with a 40 second dwell time. Helium was used as a carrier gas in both instruments and was mixed with argon from a desolvating nebuliser. The following masses were measured: ^{139}La, ^{140}Ce, ^{141}Pr, ^{146}Nd, ^{149}Sm, ^{153}Eu, ^{157}Gd, ^{159}Tb^{163}Dy, ^{165}Ho, ^{167}Er, ^{169}Tm, ^{172}Yb and ^{175}Lu and were normalized to ^{44}Ca assuming 39.7% Ca in the apatite mineral. Terbium and thulium were not analysed. NIST612, using values from (Jochum et al., 2011), was used as a standard and analysed four times per ten samples. The reproducibility of NIST612 within each analytical session was better than 10 % for each mass measured for both instruments. During LA-ICP-MS analysis, Ba oxides interfere with Eu and light (LREE) oxides interfere with the heavy (HREE) oxides (Kent and Ungerer, 2005). The rate of Ba- and LREE-oxide formation is similar to, or less than, that of Th- and U-oxides, as confirmed in a separate analytical session, and these oxides monitored during analysis were <0.3 % for UO/U and <0.6 % ThO/Th. To assess Ba-oxide interference on Eu measurements, the Ba content was measured.

Measured REE abundances were normalized against Post Archaean Average Shale (PAAS: Taylor and McLennan, 1985). Cerium anomalies were calculated arithmetically as the half sum of neighbouring elements: $Ce/Ce^* = Ce_N/(0.5Pr_N + 0.5La_N)$ (Bau and Dulski, 1996). The Eu, Pr and Y anomalies were calculated as the half sum of neighbouring elements:

$Eu/Eu^* = Eu_N/((Sm_N+Gd_N)/2)$, $Pr/Pr^* = Pr_N/ (0.5Ce_N+0.5Nd_N)$, $Y/Y^* = Y_N/((Dy_N+Ho_N)/2)$ (Byrne and Sholkovitz, 1996).

For micromorphology studies, the polished pellets were coated with a carbon conductive layer and others with a platinum one. These were then studied under a scanning electron microscope (SEM) at the University of Tartu, Estonia, using a variable pressure Zeiss EVO MA15 SEM equipped with Oxford X-MAX energy dispersive detector system (EDX) and AZTEC software for element analysis. Imaging was done both in back-scattered electron (BSE) and secondary electron (SE) modes. Over 700 micrographs were taken, some in magnifications up to 90000×.

Results

Mineralogy

Apatite-containing cores were identified during preliminary screening of measured XRD spectra. Two cores out of five core sampled were identified – GC4 from the outer shelf and 25005 from the inner shelf (Figure 1).

Core GC4 contains a high organic component, a result of horizontal transfer of organic matter originating on the inner shelf (Inthorn et al., 2006). The mineral component can be described as a calcareous phosphatic sand, containing mostly calcite, quartz, some phyllosilicates and up to 28 wt% apatite (Figure 2). The apatite content is quite stable throughout the core, rising slightly towards the bottom. Pyrite is present only in very small amounts.

The apatite can be identified by its characteristic XRD pattern as a fluor-carbonate apatite that is rather poorly crystallized as estimated by quite low values of apatite coherent stacking domain sizes averaging at about 31 nm. The unit cell parameters of apatite in this core are relatively well constrained, varying between 9.327 and 9.332 Å and 6.885 and 6.889 Å for *a* and *c* parameters, respectively (Figure 3).

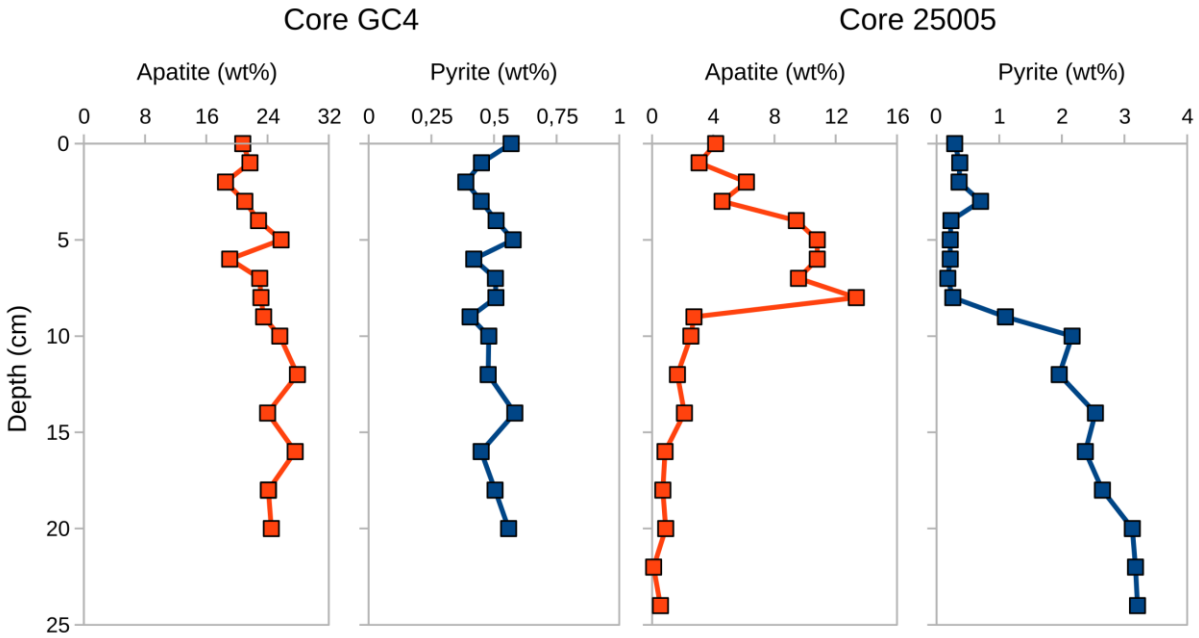

Figure 2: Apatite and pyrite content for cores GC4 and 25005, as interpreted from XRD data.

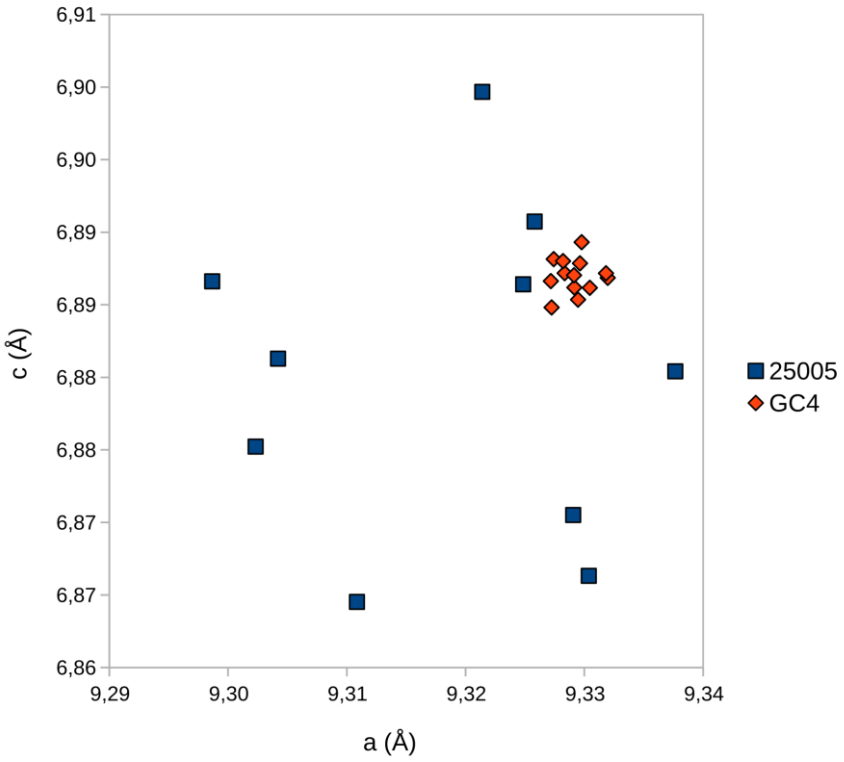

Figure 3: Apatite unit cell parameters.

Core 25005 too displays a prominent organic component along with opal diatom frustules. However, the composition of the mineral component is more varied. The core contains abundant quartz, plagioclase, phyllosilicates, pyroxene, calcite, K-feldspar, and up to 13 wt% apatite. There is a noticeable shift in mineral composition at around 8-10 cm of depth – plagioclase, phyllosilicate, pyrite and calcite component rises, while quartz, plagioclase, pyroxene and apatite content falls. Apatite starts at 4% in the topmost sediments, rises to 13% at the transition and then quickly falls to 2% and less. Pyrite is practically absent at the top, but rises to 3 wt% in the lower half of the core (Figure 2). Also in this core the apatite can be identified as a fluor-carbonate apatite that is even less crystallized as evidenced by lower value of apatite coherent stacking domain sizes averaging at about 23 nm. Interestingly, the unit cell parameters of apatite in this core had a much larger variance than in GC4 – between 9.298 and 9.337 Å and 6.865 and 6.900 Å for a and c parameters, respectively (Figure 3).

Rare earth elements

REE content within the apatite pellets was measured from seven different horizons in the 25005 core. The total REE content within pellets was heterogeneous, possibly reflecting the compositional impurities within the apatitic pellets and varied from 4 to 575 ppm without any noticeable trend respective to the depth of the samples (Figure 4). However, there is a clear and systematic difference in total REE content between the centers of the pellets and the margins (Figure 4; Figure 5). In the central parts, the total REEs were systematically lower, varying between 23 and 84 ppm.

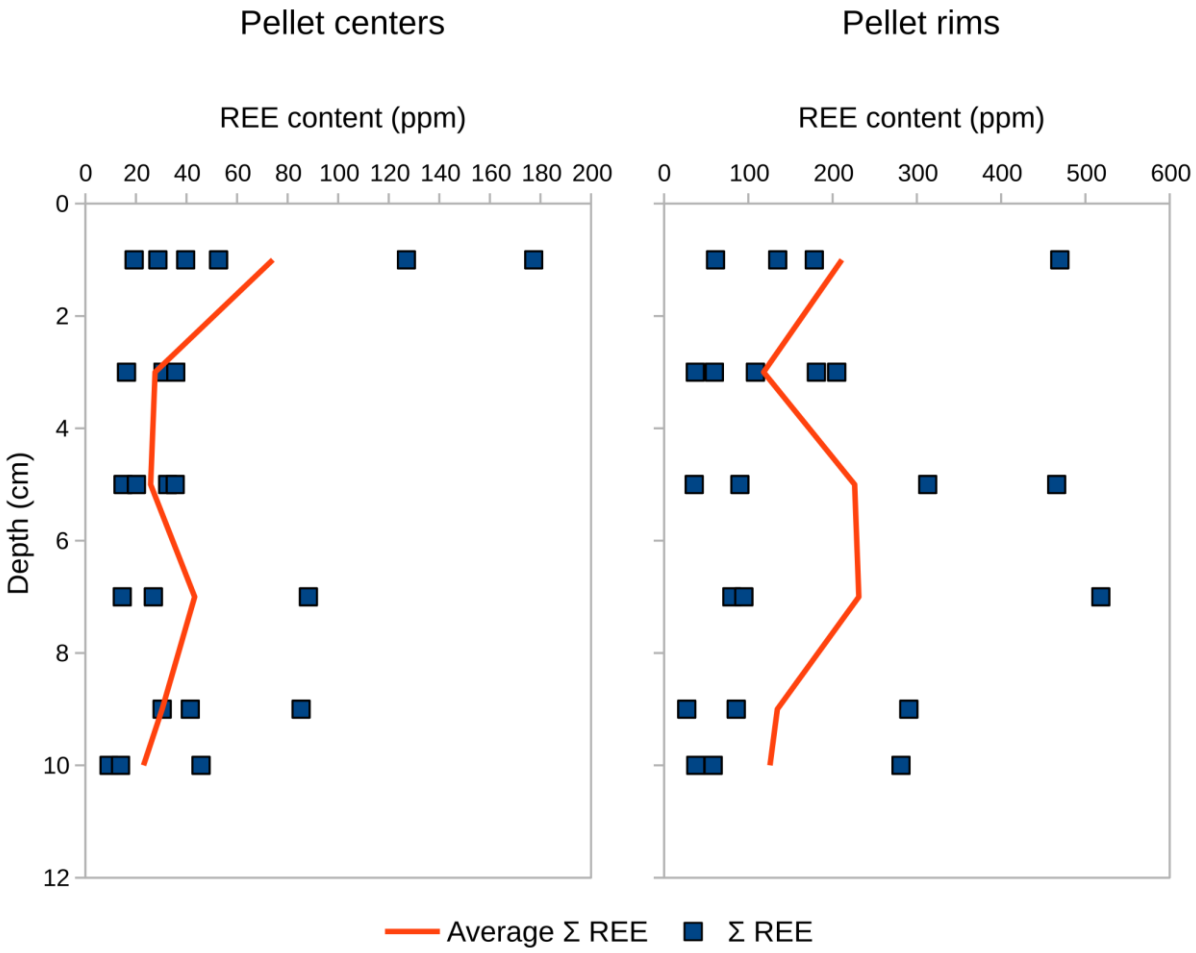

Figure 4: ∑REE content through core 25005, measured from the centers and rims of the pellets, the rims showing much higher values, but no clear trend being visible.

REE content on the rims of the pellets, however, was without exceptions significantly higher than in the center, occasionally more than 500 pm (Figure 4). Nevertheless, there is no

clearly discernible trend of total REEs with depth for pellet centers or margins. The enrichment with respect to REEs is well exemplified in line scans crossing the entire pellet (Figure 6). Importantly, the REE counts within the line scan spectra rose concurrently with the Ca and P counts on the edges of the pellet, but dropped quickly towards the centers, while Ca and P remained constant. This indicates that REE enrichment is linked to substitutions in apatite and not to some contamination on the surface of the pellets.

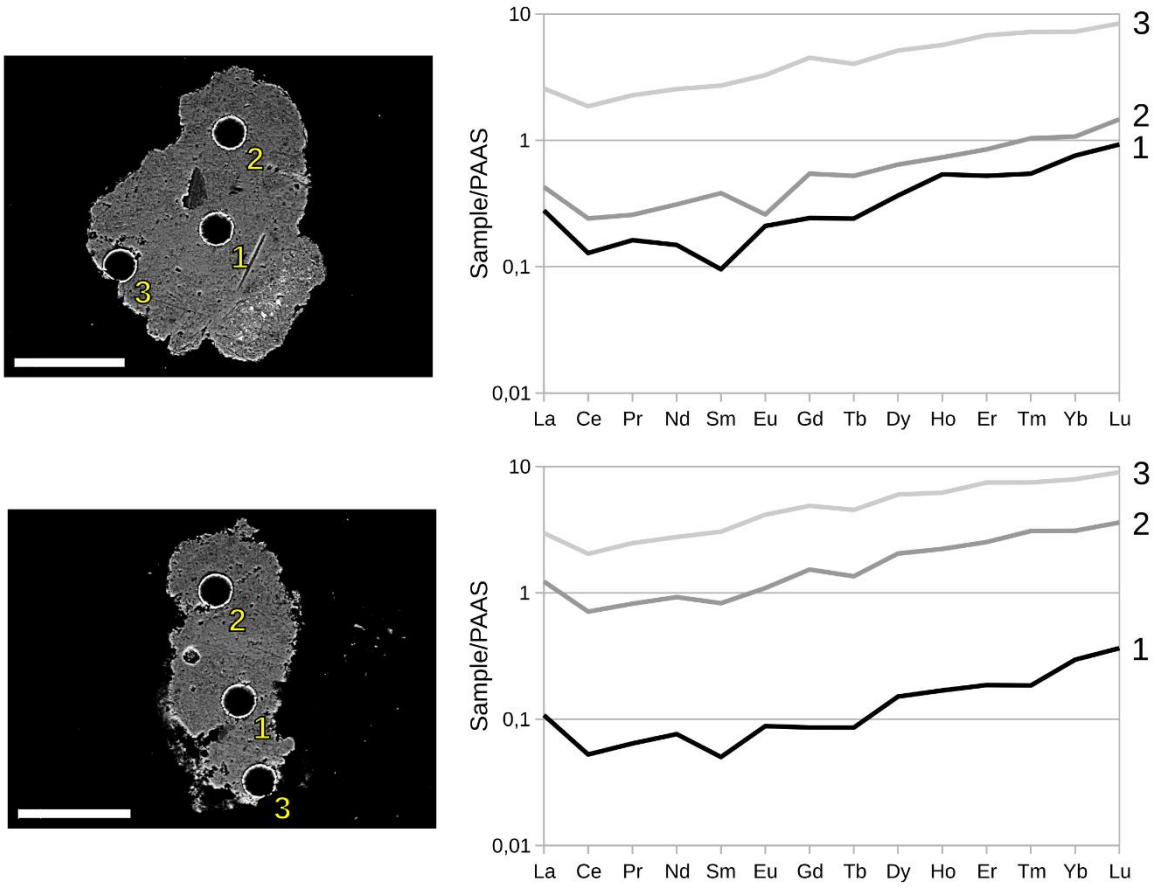

Figure 5: Heterogeneity of REE content within apatite pellets. Scale bars are 100 µm. Top pellet is from 5 cm depth, bottom from 7 cm.

The shapes of the PAAS normalized REE spectra are in good accordance with modern sea water (Reynard et al., 1999) and are consistent throughout the samples, both on the rims and in the centers of the pellets (Figure 7). The enrichment respective with seawater is up to 300 times in central parts of the pellets and up to 5000 times at the margins. The general shape of the curve represents a monotonous fall of PAAS-normalized elemental abundance from the heavy REEs towards the light REEs, with the exception of a negative Ce anomaly.

The Ce anomaly is constant throughout the core, with values ranging between 0.6 and 0.8 (Figure 8). On a La/Yb vs La/Sm graph most of samples scatter within a rather compact field, which closely resembles modern seawater ratios and suggests that the REE signal of the apatite is derived from a seawater source (Figure 9; Reynard et al., 1999).

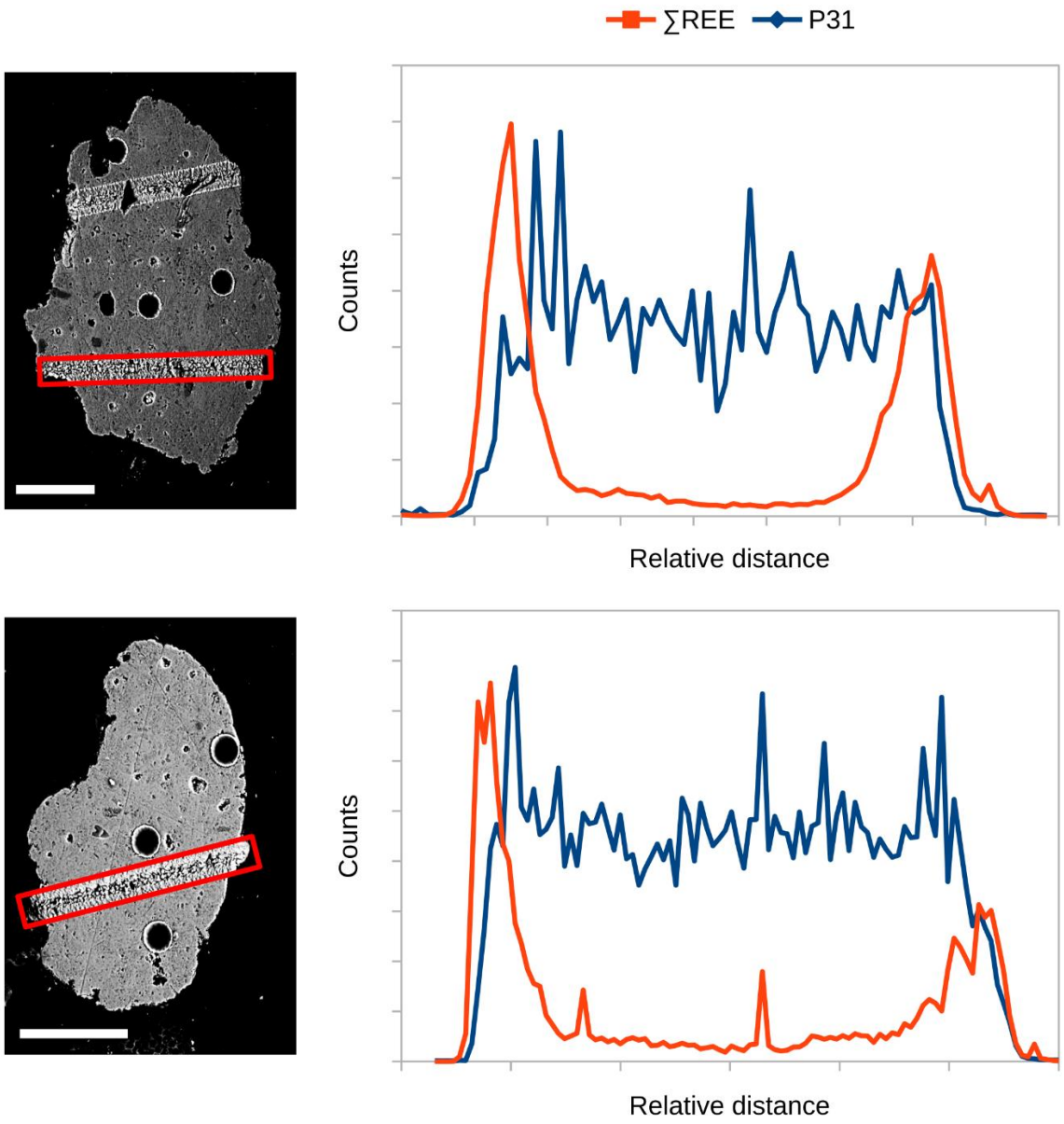

Figure 6: Line scan diagram for REE and P content. Rectangles on the pellets denote line scan ablation trails. Top pellet is from 1 cm depth, bottom from 5 cm.

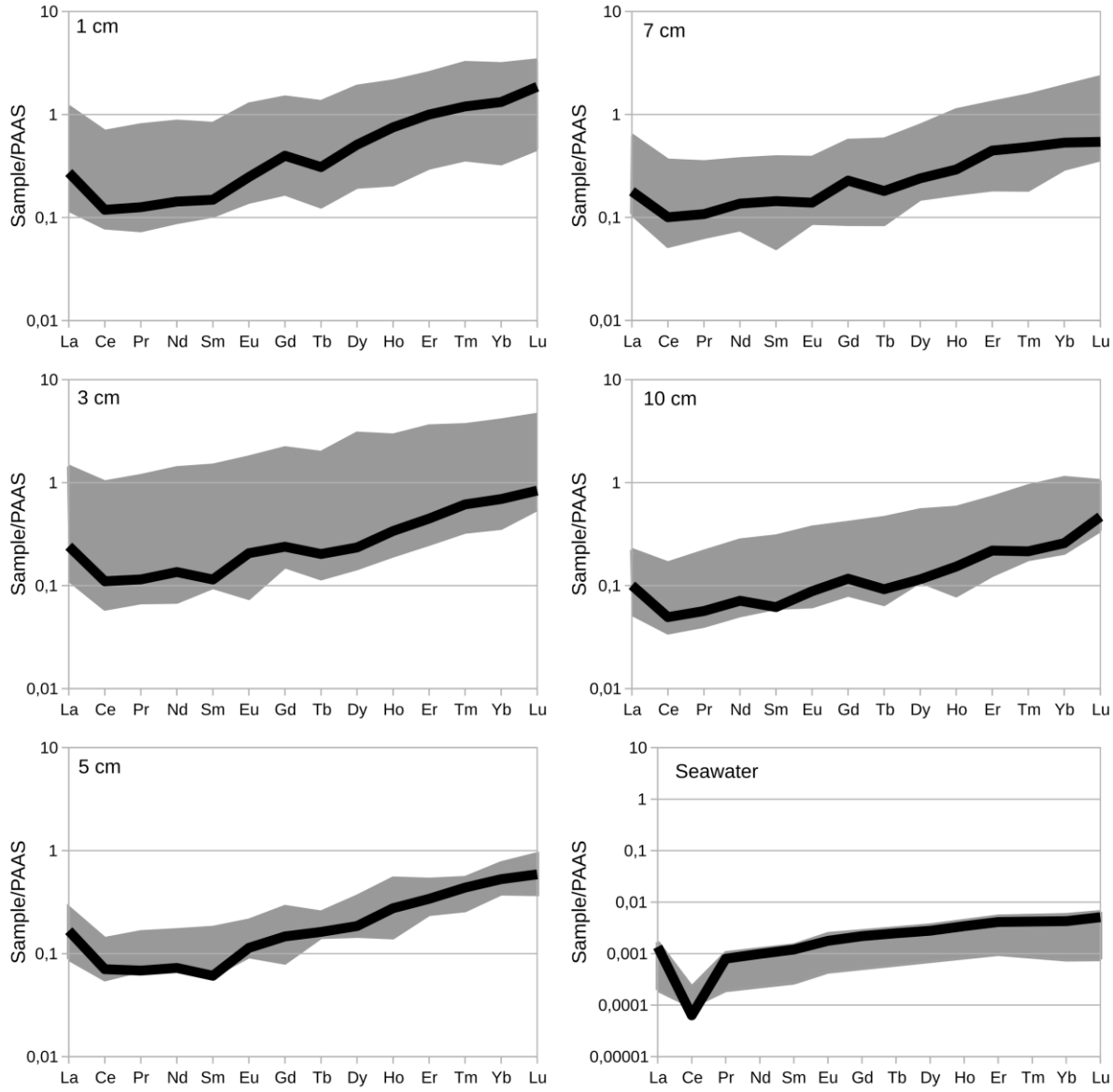

Figure 7: Variation and depth profile of REE spectra for apatite pellets from different horizons in the 25005 core. Measurements taken from the centers of the pellets. Sea water data from Reynard et. al. (1999).

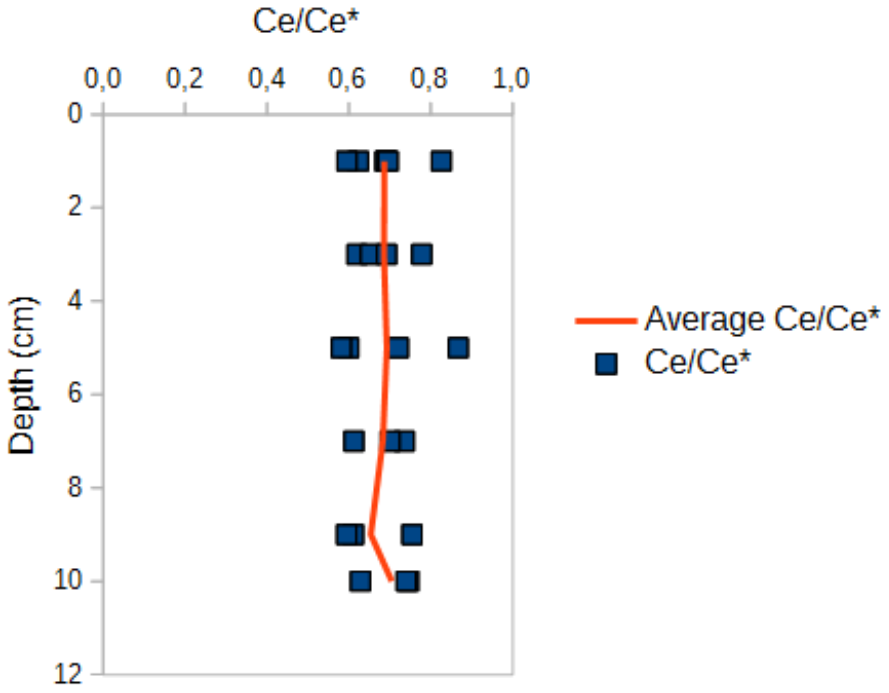

Figure 8: apatite Ce/Ce anomaly throughout the core 25005.*

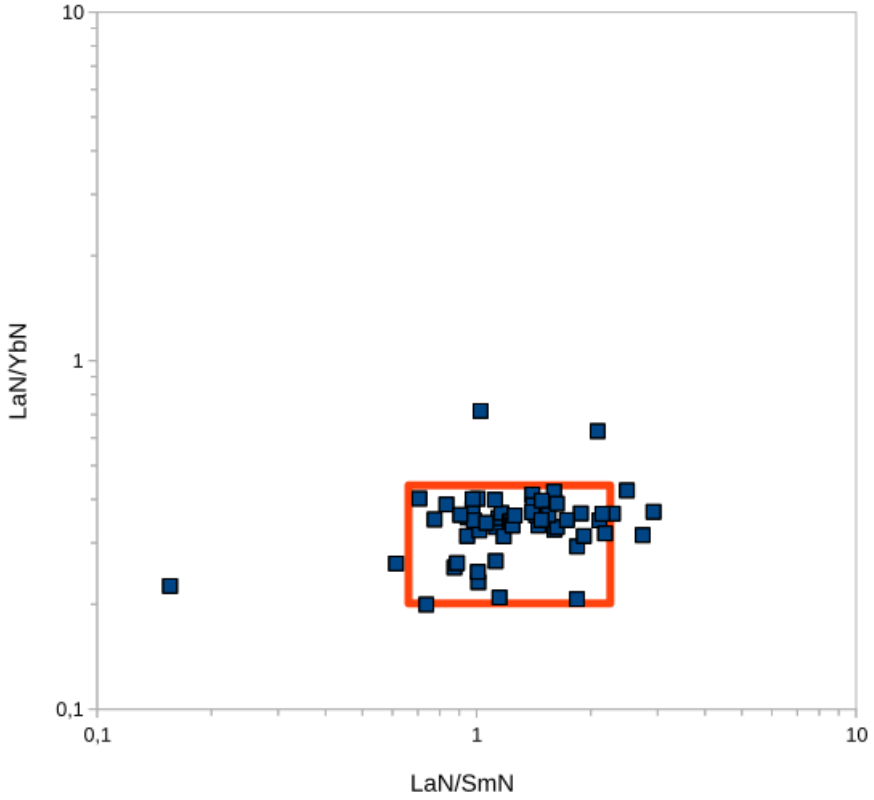

Figure 9: La/Yb vs La/Sm plot. The rectangle denotes modern seawater values, from Reynard et. al. (1999).

Microscopy

Under optical and scanning microscopy, samples from all cores were found to be dominated by “fluffy” organic matter of unknown composition and mud, which binds several mineral grains or subfossils together. In the particulate fraction, diatom frustules are relatively abundant. Aside from that, there are ostracod valves found, and other calcareous shelly fragments, quartz, feldspar and glauconite grains, a small fraction of heavy minerals and numerous apatite pellets (Figure 10a). The average grain size of the particulate fraction is typically between 100 to 300 μm.

Apatite pellets can be recognized under an optical microscope as significantly darker and slightly larger than other grains, though these are attributes shared with some glauconite grains. It is possible to distinguish them from the latter by their surface, which usually appears splotchy and pitted. Since attempts at heavy liquid fractionation turned out not to be viable, the apatite pellets examined in this study were hand-picked by visual identification, which leaves the possibility of other unidentified apatite fractions not being included in the study.

Little difference in microfabric can be discerned between pellets obtained from the shallower 25005 core and the deeper GC4 core, likewise for different horizons within the compositionally heterogeneous 25005 core. Scanning electron microscopy reveals that most of the studied apatite pellets are ca 50 to a few hundred μm in diameter, have a pitted surface, are poorly- to well-rounded and generally elongated (Figure 10b to d). The pellets have a semi-smoothed surface that usually shows numerous pores or pits. In some cases, the pellets seem to be covered by a flaky or filamentous electron-transparent layer, through which a rougher inner surface can be discerned, which gives the pellets a mottled appearance (Figure 10e and f). This layer is too thin to be able to determine its composition with an EDX measurement, but its filamentous appearance suggests that it is at least partly organic, perhaps having later phosphatized. Alternatively, the mottled surface could be topographic to a degree, perhaps a result of partial dissolution. Most of the pellets are quite porous with large pores opening to the smooth surface. The insides of the pores are much rougher and contain abundant irregular structures along with some elongated or rod-shaped aggregates (Figure 10f).

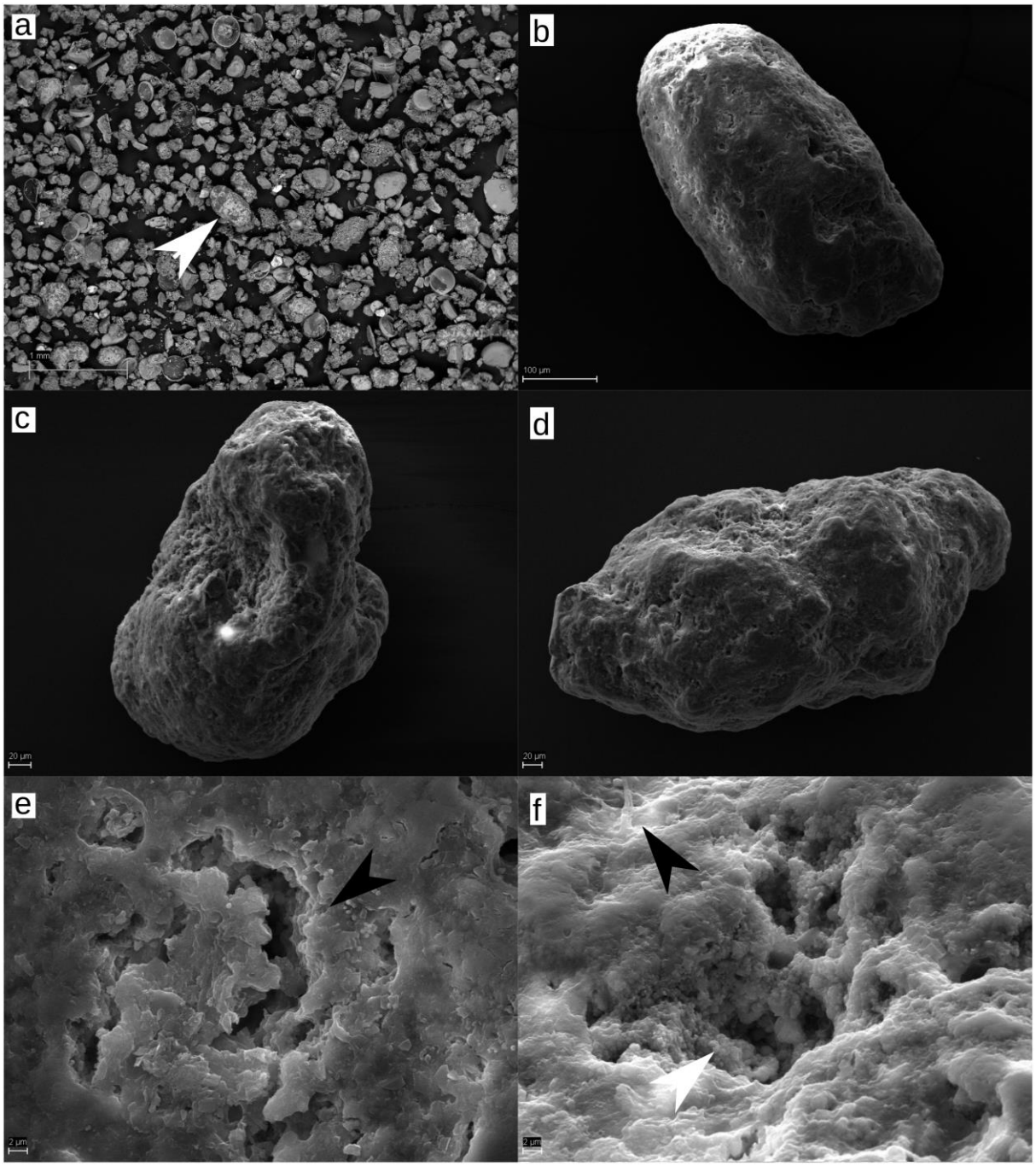

Figure 10: Apatite pellets imaged using SEM in SE mode. (a) Sediment can be described as a silty sand that contains diatom frustules, detrital grains, shell fragments and apatite pellets (denoted by white arrow). (b) to (d) Individual phosphorite pellets. These have a semi-smoothed surface, which shows numerous larger and smaller pores. (e) A flaky layer covers the pellets, denoted by arrow. Underneath, a narrow pore can be seen. (f) Filamentous parts of the covering layer (black arrow). Inside the pores are more diverse and fine-grained microstructures (white arrow).

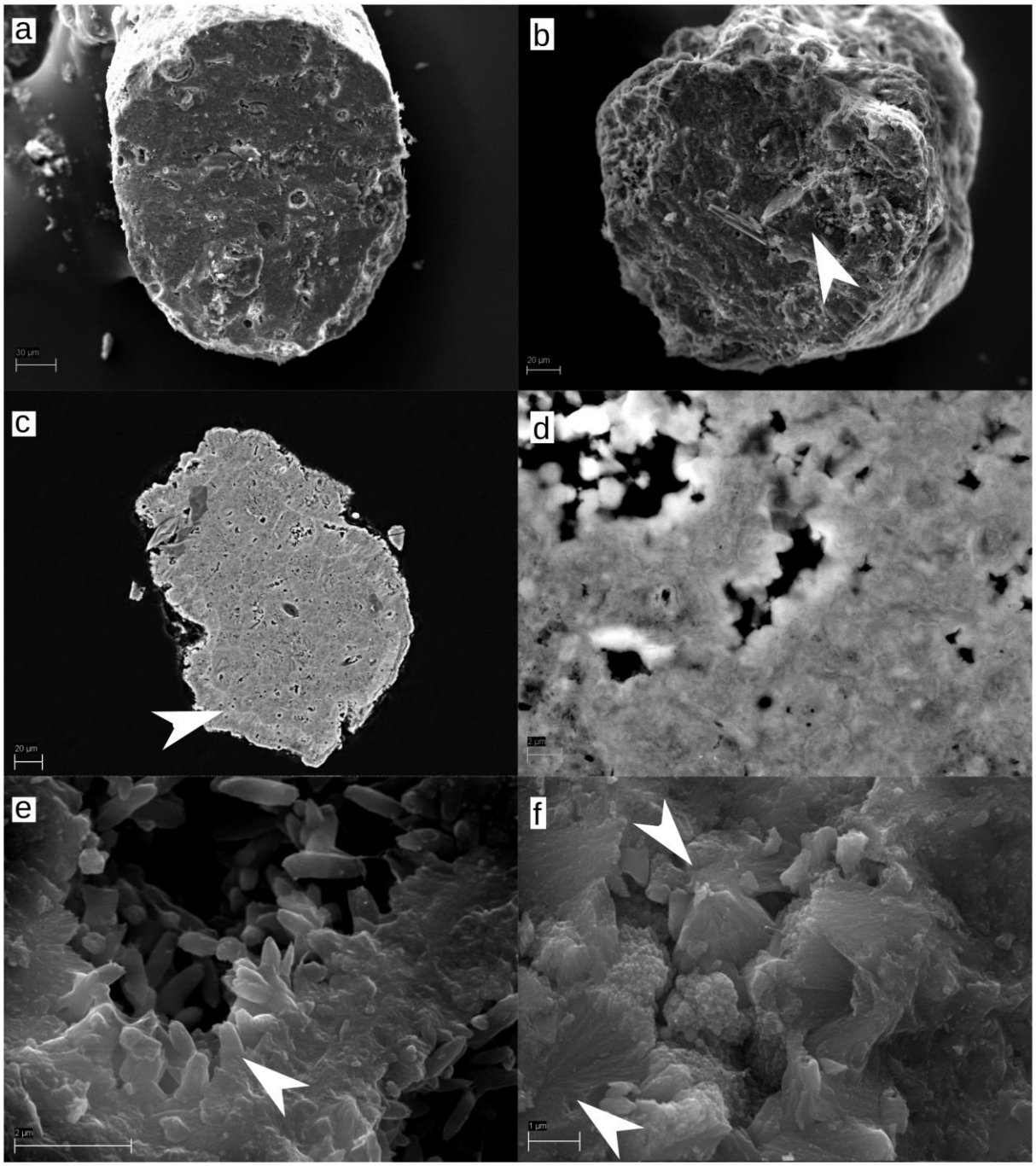

Figure 11: Inner fabric of apatite pellets. Image (c) and (d) made using SEM in BSE mode, others in SE. (a) The pellet is composed of massive apatite, but contains numerous shell fragments and pores. (b) Some pellets contain detrital grains, denoted by arrow. (c) Pellets display a distinct rim of which a section is denoted by arrow. (d) Substantial parts of the apatite matrix of the pellets are composed of intergrown rod-shaped crystallites. Wavy lines indicate separate rods. (e) Rods growing out of surrounding apatite matrix, an example denoted by arrow. (f) Apatite matrix contains numerous radial structures, denoted by arrows.

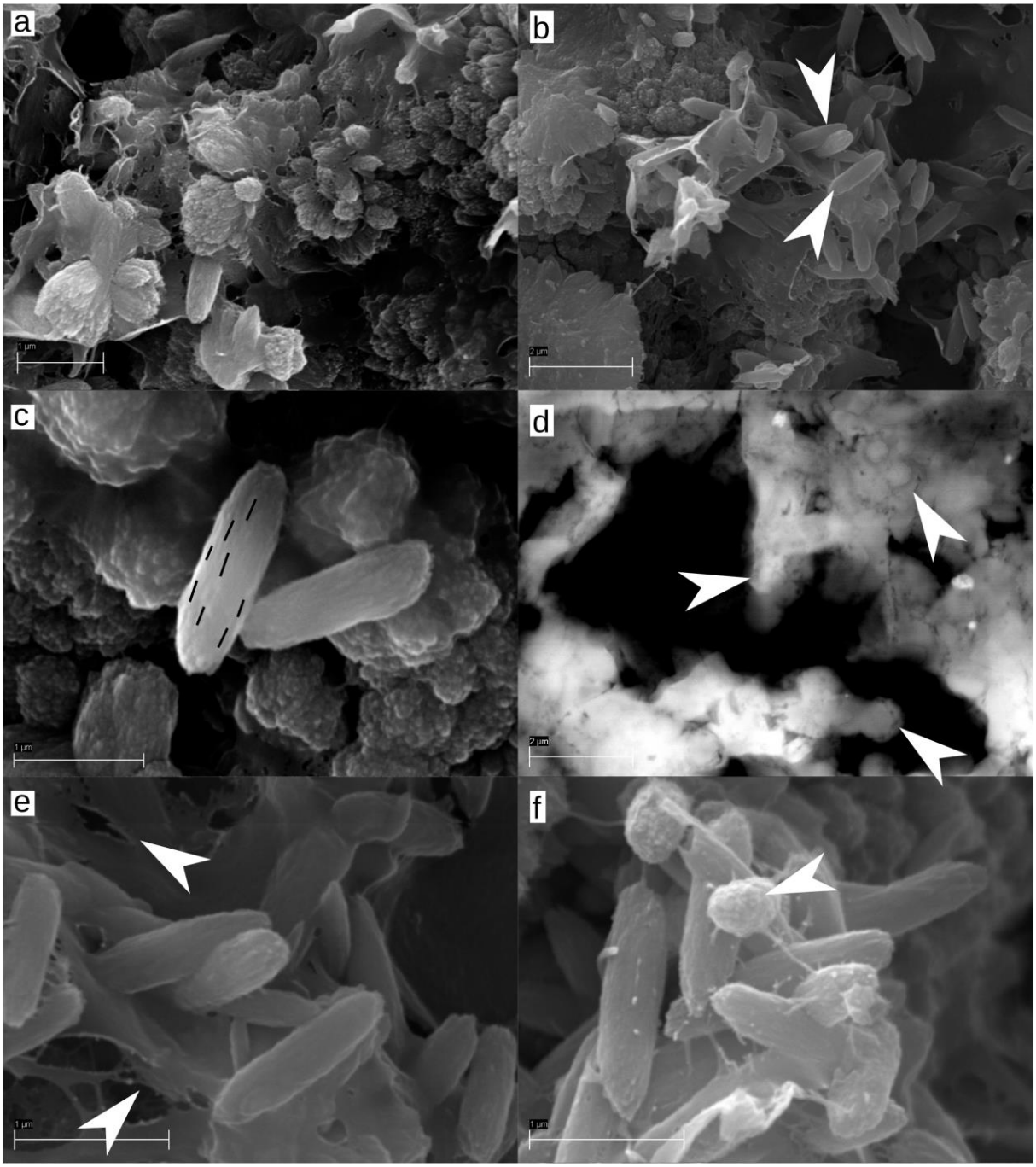

Figure 12: Microrods in apatite pellet pores, imaged with SEM in SE mode, except for (d). (a) Diverse forms of apatite microstructures. (b) Micrometer-long apatite rods cover the pore walls, some denoted by arrows. (c) High-resolution image of a single rod. Black lines denote nanocrystals oriented along the long axis. (d) BSE image of rod cross-sections. Rods denoted by arrows. A distinct core and a rim is visible. The bottommost arrow indicates a rod with an additional outer rim. (e) A film-like filamentous organic substance, denoted by arrows, is closely associated with apatite rods. (f) Collection of rods along with pyrite framboids, denoted by arrow.

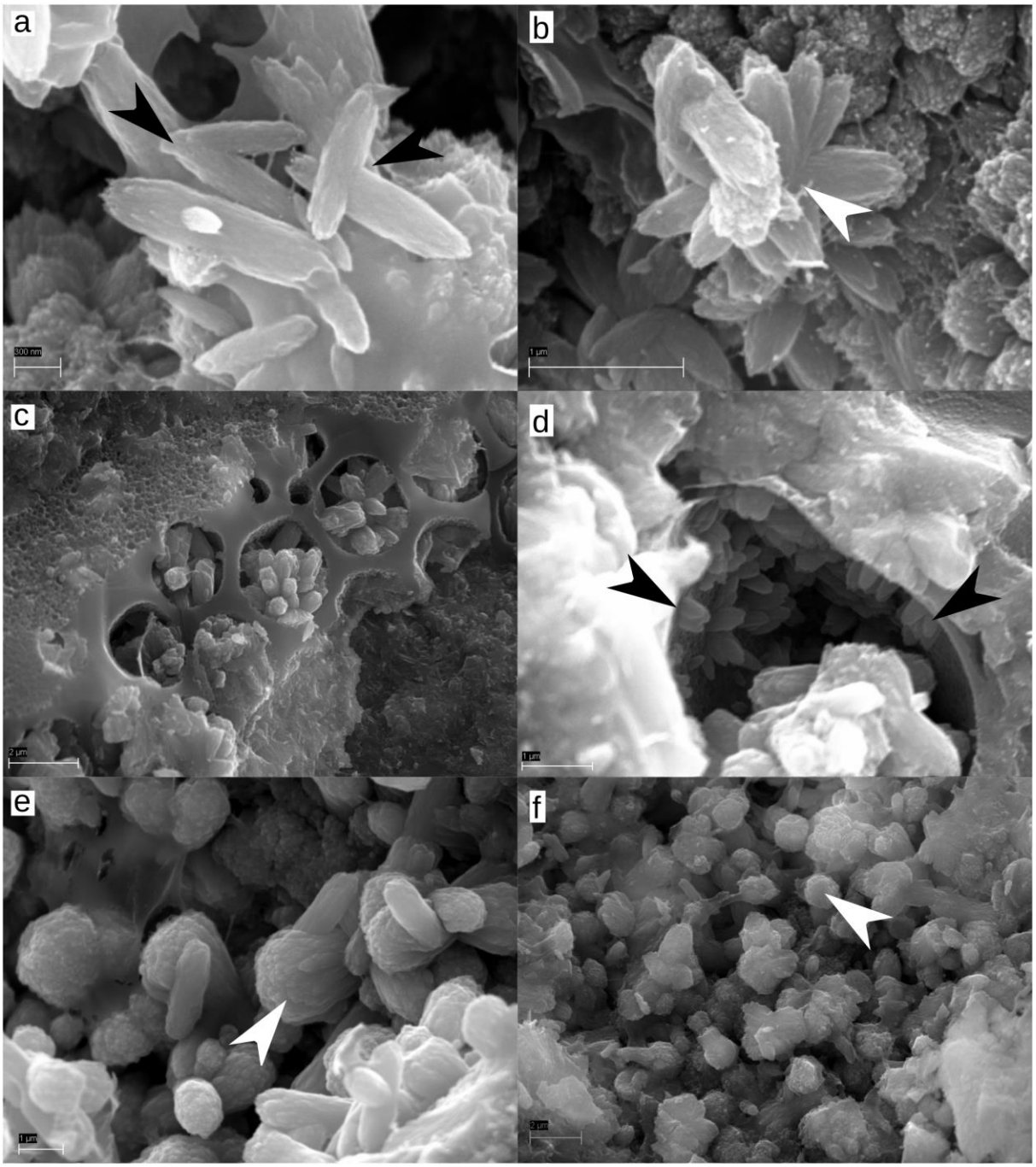

Figure 13: Apatite microstructures in pellet pores, images taken using SEM in SE mode. (a) Many apatite rods intersect with one another, intersection points marked by arrows. (b) Flower-like rod aggregate, denoted by arrow. (c) Rod aggregates inside diatom frustule fragments. (d) Truncated rods growing out of a solid shell surface denoted by arrow. (e) Dumbbell-like structures, an example denoted by arrow, are also common. (f) Semi-spherical structures, denoted by arrow.

Pellets were cut with a scalpel or ground down to reveal their inner structure. The majority of the pellets are composed of massive unstructured apatite, in which numerous pores can be found, with diameters in the tens of μm or less. Additionally, there are numerous fossil fragments – most commonly diatom frustules – and some terrigenous grains incorporated in the apatite. Some of the pores constitute either the hollow lumena or the dissolved casts of fossils (Figure 11a to b).

The massive unstructured apatite aggregate composing the pellets seems to have an irregular inner structure, with some exceptions. In BSE micrographs of polished pellets, a rim or zone of slightly differing material can be discerned around the edge of the apatite particle, ca 10-20 μm wide (Figure 11c). On a smaller scale, SE analyses reveal difficult to discern radial structures with diameters ranging from 2 to 4 μm, which permeate the apatite, especially near pores (Figure 11f).

A much more varied picture is revealed inside pores. Structures on the pore walls range from irregular or colloform, to globular, dumbbell shaped and elongated (Figure 12a). Especially conspicuous are elongated rod-shaped aggregates with rounded ends, generally ca 0.5 μm to 4 μm in length and roughly a third of that in diameter (Figure 12b to f), which are present in nearly every apatitic pellet studied. Aside from a few cases, most of the rods in any particular pore are very similar in size. Such particles co-occur with a film-like substance and are often embedded in it. Highest resolution micrographs reveal that the rods are not single crystals, but are rather composed of elongated nanocrystallites tens of nanometers in diameter, which are oriented parallel to the long axis of the rods (Figure 12c). BSE images of polished pellets reveal that the rods have a heterogeneous inner structure, with some samples displaying a core and a rim and others having an additional outer rim (Figure 12d). EDX analyses report the rods as consisting of rather pure fluoride-rich apatite, but the analysis does not to reveal any compositional differentiation inside the rods, as the BSE imaging would suggest. The rods mostly occur together with a film-like organic substance (Figure 12e). The substance permeates the pore wall wherever there are rods present, often connecting several structures as filaments or sheets. Occasionally the rods also appear together with framboidal pyrite aggregates 0.3 to 3 μm in diameter (Figure 12f).

In almost every pore, there can be found cases of rods intersecting at different angles and to different degrees (Figure 13a and b). In addition, several rods can form larger

aggregates (Figure 13 b and c). Rarely, the structures can appear truncated, growing from solid surfaces such as diatom frustules (Figure 13d). The walls of pores can often be seen to be composed of such intergrown rods (Figure 11e). Furthermore, substantial sections of the pellets can be seen to be composed of tightly intergrown rods, while other sections are more heterogeneous and stochastic in composition and fabric (Figure 11d).

Though significantly rarer, dumbbell-like structures can often be found, resembling the rods in size, but having bulged tips (Figure 13e). Furthermore, much of the pore walls are coated with larger spherical or colloform structures (Figure 13f).

Discussion

The phosphogenic system

The core GC4 sampled on Namibian shelf was taken from the outer shelf at a water depth of 301 m, south of Walvis Bay. Its location, sandy fabric, high calcite and P content and the thickness of the apatite-rich layer (Figure 2) are characteristic of the large reworked phosphate sand deposit of the middle-to-outer shelf. As suggested by the lack of pyrite, the core is at least suboxic, which makes it unlikely that phosphogenetic processes could be active, as the mechanisms facilitating phosphogenesis – such as Fe/Mn-oxide or microbial pumping – seem to all be dependent on reducing conditions or at least a nearby flux of reduced compounds (Brock and Schulz-Vogt, 2011; Ruttenberg and Berner, 1993).

Though further south of the diatomaceous ooze province occurring around Walvis Bay, nevertheless, the muddy sediments at site 25005 lie within the zone most affected by the Benguela Upwelling System and the associated high organic matter flux. At around 47 m of depth, the site is situated within the reported depth range of authigenic phosphorites (Table 1). It is shallow enough to have been periodically exposed during most of the Pleistocene (Bintanja et al., 2005), making it unlikely that the phosphorites at this site are the result of intensive transportation, as the much deeper relict phosphorite deposits of the middle to outer shelf are. Furthermore, the rapid cutoff of apatite abundance at 10 cm of depth stands in sharp contrast to the 1-2 m P-rich interval in the deeper deposit (Figure 2; Compton and Bergh, 2016). The location of the highest apatite content and its sharp decrease right on the transition to sulfidic conditions suggests that this phosphate is authigenic – a transported layer would not be expected to coincide so well with redox boundaries, as apatite is quite insoluble even in reducing conditions (Ruttenberg, 2014). XRD studies also reveal a noticeably lower crystallinity of core 25005 apatite in comparison with that in core GC4, indicating a younger origin (Figure 3). Thus, the material in core 25005 can be considered a close equivalent to the authigenic phosphorite traditionally found within the diatomaceous oozes.

The growth of phosphatic pellets

The low REE abundance of the bulk of the authigenic apatite pellets (Figure 4) has been previously reported (Baturin, 2000) and stands in stark contrast to the high REE abundance in the majority of ancient phosphorites (Joosu et al., 2015; Lécuyer et al., 2004) and also in the

reworked phosphorites of the Namibian outer shelf (Baturin, 2000). However, the REE enrichment of the rim of the pellets has not been previously shown (Figure 4 and 5). This distinct rim, revealed also from BSE micrographs (Figure 11c), is either a weathering front or a result of precipitational zonation. Phosphogenesis on the Namibian shelf is known to be episodic and zonated apatite pellets have previously been reported (Compton and Bergh, 2016). However, there is no reason the believe that the precipitation mechanisms or seawater conditions were different enough at the time of the formation of the core and the rim to result in such contrasting REE abundance, especially as the REE spectra are very similar in both cases (Figure 5). Much more likely is that the rim represents a diagenetic alteration front. Indeed, it has been previously shown that sedimentary apatite concretions, when first precipitating, are depleted in REE and get enriched only during diagenesis, showing enrichment towards their outer parts (Reynard et al., 1999).

The mostly featureless inner structure of the massive phosphate that forms the bulk of the pellets in studied material makes it difficult to discern the growth mechanism of the pellets, but at least some clues can be found near pore walls. In many cases, the apatite rods are seen growing out of pore walls, forming the pore wall itself and merging quite seamlessly into the massive apatite that forms the majority of the pellet (Figure 11e). These, along with the abundant radial cross-sections of spherical aggregates that can be seen near pore walls or in the solid matrix of the pellet (Figure 11f; see also Compton and Bergh, 2016), suggest that at least some part of the apatite matrix may be formed as a result of the intergrowth of such microstructures. This is supported by observations of polished sections of the pellets, where large areas of consolidated apatite seem to be composed of cross-sections of such rods (Figure 11d). The less-well defined apatite matrix might represent re-crystallization of (semi-) amorphous Ca-phosphate mass (Baturin, 2000).

Previous studies, which have used a wider variety of phosphatic matter, have reported poorly consolidated phosphatic concretions in the diatomaceous ooze, which they interpret as the original authigenic form (Baturin, 2000; Compton and Bergh, 2016). From the petrography of these concretions, it was suggested that they initially form as replacements of carbonaceous shells or infillings of sediment pore space (Compton and Bergh, 2016), via local rapid apatite nucleation events triggered by phosphate-cycling bacteria (Krajewski et al., 1994). Continuous organics input might provide enough P influx to promote further growth of

the already-nucleated francolite and to gradually lithify the concretions, forming the well-cemented pellets studied in this thesis (Compton and Bergh, 2016).

The controversy of the role of microbes in apatite nucleation

In natural environments, the fast-growing field of biomineralization research has provided a myriad of experimental evidence to support the importance of microbes both in providing nucleation surfaces, and in exerting more or less direct control over the precipitation of minerals via extra- or intracellular enzymes (Konhauser and Riding, 2012). Specifically, functional groups on cell walls provide suitable binding sites for calcium ions and have thus been shown to promote the nucleation of calcium minerals (Benzerara et al., 2004), though the importance of such surfaces on apatite precipitation decreases with higher degrees of supersaturation and higher speeds of precipitation (Krajewski et al., 1994).

It is not surprising then, that phosphatization is a well-known fossilization mechanism for microbes (Crosby and Bailey, 2012). Microbial fabrics have been long recognized in phosphorites and there has been extensive microstructural study of them in the decades since the introduction of scanning electron microscopy (see references in Crosby and Bailey, 2012; Krajewski et al., 1994). The rapid formation of authigenic apatite leads to the phosphatization of widely different biological structures, including nanoscale fibrous organic structures in linguliform brachiopods (Lang et al., 2016), fungal mats (Bréhéret, 1991), filamentous cyanobacteria mats, stromatolites (Krajewski et al., 1994; Rao et al., 2000), and other bacterial forms (Krajewski et al., 1994). In microbial structures the mechanism remains the same in most cases – extracellular precipitation of apatite, which tends to produce external molds of microbes (Krajewski et al., 1994). Conspicuous microbial structures have also been found in a wide variety of ancient phosphorites (Bailey et al., 2013; Cosmidis et al., 2013; Crosby and Bailey, 2012; Krajewski et al., 1994) up to and including the very earliest significant phosphorites in the world (Crosby et al., 2014; Edwards et al., 2012; Hiatt et al., 2015; Lepland et al., 2013a). The very common occurrence of phosphatized microbial cells in phosphatic sediments have been seen both as a proof of the direct role of microbial surfaces in the nucleation of phosphate minerals (Lamboy, 1990a) or as simply a consequence of the rapid precipitation of apatite, which tends to phosphatize surfaces indiscriminately (Krajewski et al., 1994).

A controversial class of phosphatic microstructures are densely-packed aggregates of small rod-shaped particles marked by rounded, non-crystalline appearance and a few μm of length, which have been reported from a variety of recent and ancient phosphorites (Baturin and Dubinchuk, 1979; Baturin, 2000; Bersenev et al., 1986; Bremner, 1980; Garrison et al., 1987; Garrison and Kastner, 1990; Lamboy, 1994, 1993; Lewy, 1990; Mullins and Rasch, 1985; O'Brien et al., 1981; Rao and Nair, 1988). In their overall outward appearance, they very much resemble phosphatized microbial mats and have been previously interpreted as such (Lamboy, 1990a, 1990b; O'Brien et al., 1981; Zanin and Zamirailova, 2011), though controversially (Baturin and Titov, 2006; Krajewski et al., 1994). Importantly, Lepland et al. (2013a) recently found very similar structures in some of the most ancient phosphorites in the world and processed them as phosphatized casts of methanotrophic archea on the basis of detailed nanostructural and geochemical study (Joosu et al., 2015; Lepland et al., 2013a; Qu et al., 2012). In the light of these findings, a more focused revision of these common microbial microstructures found in a variety of phosphorites is needed. Modern Namibian phosphorites are a prime location for such a study, as similar structures have previously been found there, along with abundant irregular and globular shapes, though previously dismissed as diagenetic precipitates (Baturin, 2002; Baturin and Titov, 2006; Compton and Bergh, 2016).

Important to bear in mind while studying phosphogenesis in the natural environment is the large body of laboratory work that has been carried out on the precipitation of apatite in the field of biomaterial research, motivated by the goal of understanding biomineralization of human bone and teeth and by possible medical applications, such as re-growing bone tissue (Vallet-Regí and González-Calbet, 2004). Since controlled biomineralization in vertebrates takes place in a complex environment of organic scaffolds and catalysts, this research has focused on the effects of polymers as nucleation templates or additives, while also keeping in mind the effect of inorganic additives, pH and temperature (Bleek and Taubert, 2013). These studies have shown an exceedingly diverse picture of the possible apatite mineral forms capable of being grown via the large variety of developed synthesis methods (Lin et al., 2014). Densely-packed rod-shaped particles are an often seen result of such experiments (Ruan et al., 2013), these are also well-known among the equally-variable calcite precipitates (Meldrum and Cölfen, 2008; Meldrum and Hyde, 2001).

The nature of the apatite microrods in Namibian phosphate pellets

The dense collections of apatitic rods that appear ubiquitous within the pores of the Namibian phosphate bear a strong superficial resemblance to microbial biofilms, due to their generally similar sizes, noncrystalline appearance and co-occurrence within organic films that closely resemble microbial exopolymeric substances (Figure 12). Very similar fabrics have been found in other ancient and recent phosphorites and have previously been interpreted by some authors as aggregations of microbial casts (Lamboy, 1990a; Zanin and Zamirailova, 2011). Their formation mechanism was hypothesized to be the nucleation of apatite nanocrystals on microbial walls, which are known to provide suitable binding sites for biologically induced mineral formation (Benzerara et al., 2004). The minerals encrusting the microbes then start to grow and coalesce, until the organic structures are wholly replaced by apatite (Lepland et al., 2013a). There are, however, significant problems with this interpretation in the case of the phosphorites of the Namibian margin, some of which have also been pointed out in previous studies of Namibian material (Baturin and Titov, 2006). Firstly, very many of the rods seem to intersect one another, examples of which can be found almost in every pore (Figure 13a and b). While this could possibly be the result of post-nucleation growth of what were originally much smaller and non-intersecting apatite aggregates, the in-plane intertwinning of many of the rods makes it very unlikely that they were originally bacterial cells and points to mineral twinning as a more likely scenario. While the rods are mostly of similar size within a single pore, there exists a large variation in sizes between different pores, which would not be expected in the case of bacteria. Furthermore, some cases of co-occurrence of larger and smaller rods have been found (Figure 13e). The truncated forms growing off of solid surfaces are also hard to reconcile with a bacterial origin (Figure 13d).

The growth of very similar apatite forms have been previously reported in laboratory experiments conducted at high supersaturations for the purpose of elucidating phosphorite origin (van Cappellen and Berner, 1991), and, much more commonly, for the purpose of testing biomineralization processes and for developing medical applications (Ruan et al., 2013). An important aspect for understanding the genesis of such apatite microstructures is the occurrence of different types of microstructures in these pores: rods with bulged tips, dumbbells and semi-spherical aggregates (Figure 14). A similar assemblage of microstructures has been reported to occur in double-diffusion experiments in a variety of

organic substrates (Busch et al., 1999; Kniep and Busch, 1996; Kniep and Simon, 2006; Wu et al., 2010). During growth, these fluoroapatite-gelatine nanocomposites start out as hexagonal, rod-shaped, or spindle-shaped seed crystals, which then start to bulge at their tips, forming dumbbells and eventually enclosing into a spherical form (Figure 15). This unusual form of crystal growth has been found to be controlled by an intrinsic dipolic field generated by organic macromolecules that are incorporated in the nanostructure of the aggregate (Simon et al., 2006). A very similar form of crystal growth is interpreted to have formed the succession of rod-shaped to dumbbell to spherical or radial microstructures found on the Namibian shelf, though Baturin (2000) has offered alternative hypotheses for the formation of spherical/radial aggregates. In addition to the very similar morphology, the rods appear almost without exception in association with an organic substrate, the likes of which is generally needed for the formation of the fluoroapatite-gelatine nanocomposites.

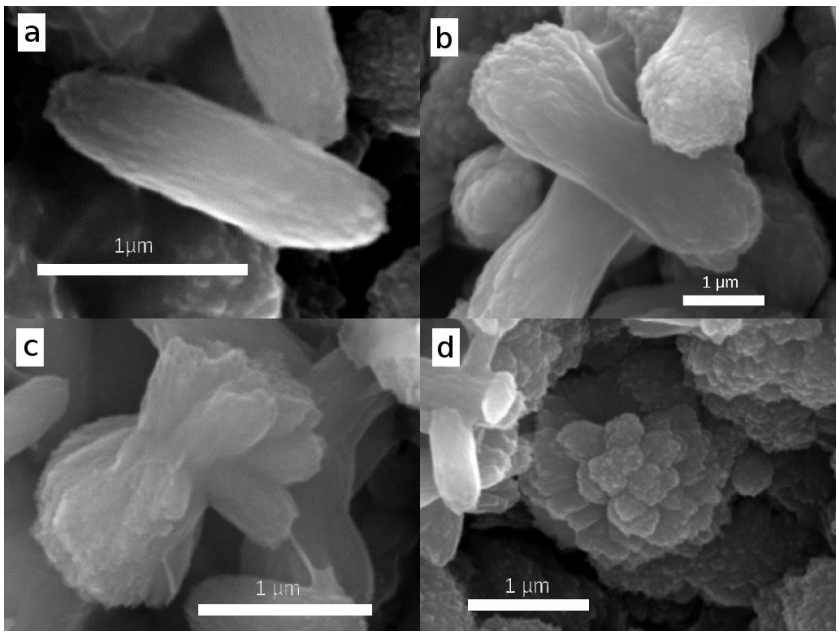

Figure 14: Apatite rods along with other microstructures form a continuum from (a) spindle-shaped elongated rods to (b) rods that start to bulge at their tips to (c) dumbbells to (d) spherical aggregares.

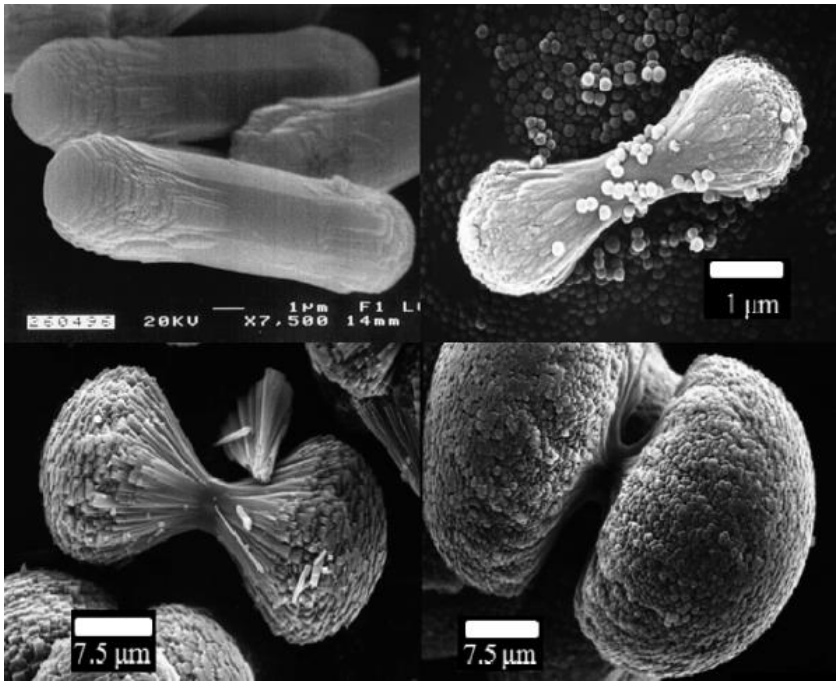

Figure 15: Fluoroapatite-gelatine nanocomposites display growth patterns similar to the apatitic microstructures of the Namibian phosphorites. Modified after (Busch et al., 1999; Wu et al., 2010).

The reason why dumbbell-like structures are not as common in the Namibian samples as they can be in laboratory experiments are the relatively small pore spaces in the phosphorite pellets and the dense nucleation of the seed crystals, which means that most of the rods start to intergrow before they reach the dumbbell or spherical stages.

The role of microbes in the formation of Namibian phosphorite

Krajewski et al. (1994), along with many researchers expressed a skepticism of all putative bacterial forms in phosphorites (except filamentous cyanobacteria and fungi) and believed that only the specific microfossil morphologies that have been experimentally demonstrated can be taken seriously. Such forms are mainly empty or partially infilled coccoid to rod-shapes, in essence the forms which contain hollow lumena (Cosmidis et al., 2013). The present study gives further credence to such skepticism. However, even though the abundant microstructures in themselves might not be fossilized bacteria, there is still evidence within these phosphorites of a significant influence of bacteria on their formation.

Slightly negative Ce/Ce* anomalies indicate that the formation environment was at least suboxic (Figure 8; Liu et al., 1988). Abundant glauconite present within both cores is

commonly associated with fluctuating redox conditions (Stille and Clauer, 1994; Wigley and Compton, 2007). These conditions are favorable to the sulfide-oxidizing microbial communities thought to be responsible for inducing phosphogenesis on the Namibian shelf (Schulz and Schulz, 2005). More directly relevant is the presence of abundant framboidal pyrite tightly embedded within the microstructure of the apatite, commonly associated with microbial S-cycling (Figure 12f). An integral part of most phosphorites are traces of bacterially influenced organic compounds (Krajewski et al., 1994). One tantalizing clue to the influence of bacteria on phosphogenesis at the Namibian margin is the ubiquitous organic substance permeating the pore walls and co-occurring with apatitic rods within the phosphatic pellets (Figure 12e). Such a substance most likely results from microbial activity, perhaps a product of microbial breakdown of sedimentary organic matter or possibly a relict of bacterially excreted exopolymeric substance. A clear understanding of the chemical nature of this substance is outside of the scope of this study, but the close relationship between it and the apatite rods gives reason to speculate that this substance serves as a common or even primary nucleation substrate during the formation of these microstructures. Microbially produced organic substances are after all well known to act as a nucleation templates for many different kinds of biominerals (Konhauser and Riding, 2012). If the apatite microstructures do represent analogs of fluoroapatite-gelatine nanocomposites, the importance of this substance is rather evident. Thus, the ever-increasing understanding of the critical role of microbes in facilitating phosphorite formation can possibly be extended to the most enigmatic part of this process: the nucleation of authigenic apatite.

The question of the Namibian phosphorites' origin is made more important by their striking similarity to the ones found in ancient phosphorites, including some of the earliest (Lepland et al., 2013a), and that they have been used to make paleoenvironmental inferences based mostly on their morphology. Thus it is important to understand the nature and origin of modern phosphorite microfabric. Especially important in this might be TEM-studies of the nanostructure of these rods, which has been documented extensively in the case of fluoroapatite-gelatine nanocomposites (Brickmann et al., 2010).

Conclusions

Phosphorites are a crucial component of the global phosphorous cycle, and globally important for the production of fertilizers. Phosphorites also have great potential to be used as paleoenvironmental proxies, owing to their unique temporal distribution, and have already been used as such. This depends, however, on an incomplete understanding of their origin. There is an ever-increasing awareness of the significant role of microbes in the formation of phosphorites, especially of sulfur and polyphosphate metabolizing bacterial communities. In this thesis the nucleation and primary growth of apatite minerals in the natural environment and its possible relation to microbial processes was studied.

A set of cores was retrieved from the sediments of the shelf sea off the coast of Namibia, an area known for modern phosphogenesis. Of the two P-rich cores, one was found to contain reworked and concentrated pre-Holocene phosphorite, while the other hosted authigenic apatite pellets, as inferred mainly by the association of a well-defined redox zone with a peak in apatite content. Furthermore, the pellets were revealed to have a REE-rich alteration rim and a REE-poor center, reminiscent of authigenic apatite in the first stages of diagenesis.

The apatite pellets are composed of massive carbonate fluoroapatite interspersed with detrital debris and skeletal fragments. These also contain numerous micropores, which in turn host a variety of apatite microstructures. Most ubiquitous of these are ca 1 μm elongated rods with rounded tips, which seem to form large parts of the pellets. These structures strongly resemble phosphatized microbial films, especially as they co-occur with an organic matrix. However, the rods tend to intersect one another, very reminiscently of mineral twinning. Bulged forms, dumbbells and spherical aggregates form a growth continuum with the rods as starting points. A very similar succession of apatite microstructures, called fluoroapatite-gelatine nanocomposites, have previously been reported from laboratory experiments carried out at high supersaturations in organic matrices. Therefore the apatite rods from Namibian phosphorite pellets can be interpreted to be analogous to these nanocomposites.

The abiological nature of the apatite rods urges caution when interpreting similar structures as fossilized microbes, as has been done in the case of both recent and ancient phosphorites. Nevertheless, the ubiquitous organic matrix, likely a bacterial byproduct, might serve as the main template for the nucleation of apatite and thus still speaks to the importance of microbes on the very first stages of phosphorite formation.

Retsentsete Namiibia šelfimere fosforiitide geokeemia, mikrostruktuur ja päritolu

Fosforiidid on olulised komponendid maailma fosforiringes ja kriitilise tähtsusega ressursid väetiste tootmisel. Samas ei mõisteta teatud aspekte fosforiitide tekkemehhanismist veel sugugi hästi. Hiljuti on järjest enam maad võtnud arusaam mikroobide olulisest rollist fosforiitide tekke indutseerimisel. Käesolevas töös uuriti võimalikke mikrobiaalse mõju väljendusi apatiidi nukleerumisel ja esmasel kasvul kaasaegsetes fosforiitides.

Namiibia šelfimere setetes, kust võeti antud töös kasutatud settesüdamikud, leiab aset tänapäevane fosforiitide teke. Kahest fosfaadirikkast settesüdamikust üks esindas Holotseeni eelset edasikantud ja kontsentreeritud fosfaatset liiva. Teises aga leidusid autigeensed apatiiditerad, mille kontsentratsioonimaksimum langes kokku redokstingimuste üleminekuga. Terade ääred olid rikastunud haruldastest muldmetallidest, keskmed aga vaesustunud, mis viitasid varadiageneetilistele ümberkristalliseerumisle.

Apatiitsed terad koosnevad massiivsest apatiidist, milles esinevad mikropoorid. Mikropooride siseseinu katavad arvukad struktuurid, millest kõige levinumad on piklikud ja ümardatud otstega, ca 1 µm pikkused apatiitsed pulgakesed. Sellised pulgakesed moodustavad suure osa kogu terast. Tänu nende püsivatele suurustele ja nende tihedale seotusele filamentse orgaanilise massiga meenutavad nad fosfatiseerunud mikrobiaalseid biokilesid. Samas on paljud sellised pulgakesed üksteisest läbi kasvanud, moodustades seejuures kas 90° või 60° lõikuvaid läbikasvestruktuure, mis on omased pigem abioloogilisele mineraalsetele kasvule. Samuti näivad pulgakesed olevat vaid esimene osa pikemast kristallikasvu reast: ühes nendega esineb ka hulgaliselt hantlikujulisi ja sfäärilisi struktuure. Sarnast üleminekut on varem täheldatud ka laborieksperimentides, nn. fluoroapatiidi-gelatiini nanokomposiitide puhul, kus Ca-fosfaadi väljasettimisel orgaanilises matriitsis moodustusid algul pulgakesed, edasi hantlid ja lõpuks sfäärilaadsed vormid. Sellisel juhul võiksid Namiibia fosforiitides leiduvad mikrostrkuurid olla anloogsed nende abiogeensete nanokomposiitidega.

Kuna selliseid mikrostruktuure on leitud paljudest retsentsetest ja iidsetest fosforiitidest, tasuks ümber hinnata morfoloogiale tuginevad interpretatsioonid taoliste struktuuride päritolust. Nende apatiidivormidega tugevalt seotud orgaaniline substants on aga tõenäoliselt bakteriaalse metabolismi kõrvalprodukt ning mängib suurt rolli apatiidi nukleerumisel, mis viitab mikroobide tähtsusele fosforiitide tekke esmaetappidel.

Acknowledgments

I would like to thank my supervisors Kalle Kirsimäe, Aivo Lepland and Jake Bailey for introducing me to the wonderful subject of phosphogenesis and for their thorough help at every step in my master's project.

I also thank Päärn Paiste for providing the great ICP-MS results, the organizers, students and funders of the RGNO 2015 course in Henties Bay, Namibia, for an incredibly enlightening summer school and the crew and scientific staff of the wonderful R/V Mirabilis.

References

Alsenz, H., Illner, P., Ashckenazi-Polivoda, S., Meilijson, A., Abramovich, S., Feinstein, S., Almogi-Labin, A., Berner, Z., Püttmann, W., 2015. Geochemical evidence for the link between sulfate reduction, sulfide oxidation and phosphate accumulation in a Late Cretaceous upwelling system. Geochem. Trans. 16. doi:10.1186/s12932-015-0017-1

Arning, E.T., Birgel, D., Brunner, B., Peckmann, J., 2009. Bacterial formation of phosphatic laminites off Peru. Geobiology 7, 295–307. doi:10.1111/j.1472-4669.2009.00197.x

Arning, E.T., Birgel, D., Schulz-Vogt, H.N., Holmkvist, L., J∅rgensen, B.B., Larson, A., Peckmann, J., 2008. Lipid Biomarker Patterns of Phosphogenic Sediments from Upwelling Regions. Geomicrobiol. J. 25, 69–82. doi:10.1080/01490450801934854

Bailey, J.V., Corsetti, F.A., Greene, S.E., Crosby, C.H., Liu, P., Orphan, V.J., 2013. Filamentous sulfur bacteria preserved in modern and ancient phosphatic sediments: implications for the role of oxygen and bacteria in phosphogenesis. Geobiology 11, 397–405. doi:10.1111/gbi.12046

Bailey, J.V., Joye, S.B., Kalanetra, K.M., Flood, B.E., Corsetti, F. a, 2007. Evidence of giant sulphur bacteria in Neoproterozoic phosphorites. Nature 445, 198–201. doi:10.1038/nature05457

Bailey, J.V., Salman, V., Rouse, G.W., Schulz-Vogt, H.N., Levin, L. a, Orphan, V.J., 2011. Dimorphism in methane seep-dwelling ecotypes of the largest known bacteria. ISME J. 5, 1926–35. doi:10.1038/ismej.2011.66

Baturin, G., Dubinchuk, V., 1979. Microstructures of Oceanic Phosphorites. Atlas Microphotographs Mosc. Nauka.

Baturin, G.N., 2002. Nodular Fraction of Phosphatic Sand from the Namibia Shelf. Lithol. Miner. Resour. 37, 1–17. doi:10.1023/A:1013628020381

Baturin, G.N., 2000. Formation and Evolution of Phosphorite Grains and Nodules on the Namibian Shelf, From Recent to Pleistocene. Spec. Publ. SEPM.

Baturin, G.N., 1971. Stages of Phosphorite Formation on the Ocean Floor. Nature 232, 61–62. doi:10.1038/10.1038/physci232061a0

Baturin, G.N., Bezrukov, P.L., 1979. Phosphorites on the sea floor and their origin. Mar. Geol. 31, 317–332. doi:10.1016/0025-3227(79)90040-9

Baturin, G.N., Titov, A.T., 2006. Biomorphic formations in recent phosphorites. Oceanology 46, 711–715. doi:10.1134/S0001437006050110

Bau, M., Dulski, P., 1996. Anthropogenic origin of positive gadolinium anomalies in river waters. Earth Planet. Sci. Lett. 143, 245–255. doi:10.1016/0012-821X(96)00127-6

Benzerara, K., Menguy, N., Guyot, F., Skouri, F., de Luca, G., Barakat, M., Heulin, T., 2004. Biologically controlled precipitation of calcium phosphate by Ramlibacter tataouinensis. Earth Planet. Sci. Lett. 228, 439–449. doi:10.1016/j.epsl.2004.09.030

Bersenev, I., Baturin, G., Lelikov, E., Gusev, V., 1986. Neogene phosphorites of the Sea of Japan. Phosphate Depos. World Vol. 3 Neogene Mod. Phosphorites 156, 167.

Bintanja, R., van de Wal, R.S.W., Oerlemans, J., 2005. Modelled atmospheric temperatures and global sea levels over the past million years. Nature 437, 125–128. doi:10.1038/nature03975

Bleek, K., Taubert, A., 2013. New developments in polymer-controlled, bioinspired calcium phosphate mineralization from aqueous solution. Acta Biomater. 9, 6283–6321. doi:10.1016/j.actbio.2012.12.027

Bréhéret, J.-G., 1991. Phosphatic concretions in black facies of the Aptian-Albian Marnes bleues Formation of the Vocontian basin (SE France), and at site DSDP 369: evidence of benthic microbial activity. Cretac. Res. 12, 411–435. doi:10.1016/0195-6671(91)90018-8

Bremner, J.M., 1980. Concretionary phosphorite from SW Africa. J. Geol. Soc. 137, 773–786. doi:10.1144/gsjgs.137.6.0773

Brickmann, J., Paparcone, R., Kokolakis, S., Zahn, D., Duchstein, P., Carrillo-Cabrera, W., Simon, P., Kniep, R., 2010. Fluorapatite-Gelatine Nanocomposite Superstructures: New Insights into a Biomimetic System of High Complexity. ChemPhysChem n/a-n/a. doi:10.1002/cphc.201000232

Brock, J., Schulz-Vogt, H.N., 2011. Sulfide induces phosphate release from polyphosphate in cultures of a marine Beggiatoa strain. ISME J. 5, 497–506. doi:10.1038/ismej.2010.135

Burnett, W.C., 1977. Geochemistry and origin of phosphorite deposits from off Peru and Chile. Geol. Soc. Am. Bull. 88, 813–823. doi:10.1130/0016-7606(1977)88<813:GAOOPD>2.0.CO;2

Burnett, W.C., Glenn, C.R., Yeh, C.C., Schultz, M., Chanton, J., Kashgarian, M., 2000. U-series, 14C, and stable isotope studies of recent phosphatic “protocrusts” from the Peru margin. Mar. Authigenesis Glob. Microb. 66, 163–183. doi:10.2110/pec.00.66.0163

Busch, S., Dolhaine, H., DuChesne, A., Heinz, S., Hochrein, O., Laeri, F., Podebrad, O., Vietze, U., Weiland, T., Kniep, R., 1999. Biomimetic morphogenesis of fluorapatite-gelatin composites: fractal growth, the question of intrinsic electric fields, core/shell assemblies, hollow spheres and reorganization of denatured collagen. Eur. J. Inorg. Chem. 1999, 1643–1653.

Byrne, R.H., Sholkovitz, E.R., 1996. Chapter 158 Marine chemistry and geochemistry of the lanthanides, in: Earths, B.-H. on the P. and C. of R. (Ed.). Elsevier, pp. 497–593.

Cárdenas, A.L., Harries, P.J., 2010. Effect of nutrient availability on marine origination rates throughout the Phanerozoic eon. Nat. Geosci. 3, 430–434. doi:10.1038/ngeo869

Carr, M.-E., 2001. Estimation of potential productivity in Eastern Boundary Currents using remote sensing. Deep Sea Res. Part II Top. Stud. Oceanogr., The US JGOFS Synthesis and Modeling Project: Phase 1 49, 59–80. doi:10.1016/S0967-0645(01)00094-7

Coles, S.K.P., Wright, C.I., Sinclair, D.A., Bossche, P.V. den, 2002. The Potential for Environmentally Sound Development of Marine Deposits of Potassic and Phosphatic

Minerals Offshore, Southern Africa. Mar. Georesources Geotechnol. 20, 87–110. doi:10.1080/03608860290051822

Compton, J.S., Bergh, E.W., 2016. Phosphorite deposits on the Namibian shelf. Mar. Geol. doi:10.1016/j.margeo.2016.04.006

Compton, J.S., Mallison, D., Glenn, C.R., Filippelli, G.M., Föllmi, K.B., Shields, G., Zanin, Y., 2000. Variations in the global phosphorus cycle, in: Marine Authigenesis: From Global to Microbial. SEPM Special Publication, pp. 21–34.

Compton, J.S., Mulabisana, J., McMillan, I.K., 2002. Origin and age of phosphorite from the Last Glacial Maximum to Holocene transgressive succession off the Orange River, South Africa. Mar. Geol. 186, 243–261. doi:10.1016/S0025-3227(02)00211-6

Compton, J.S., Wigley, R., McMillan, I.K., 2004. Late Cenozoic phosphogenesis on the western shelf of South Africa in the vicinity of the Cape Canyon. Mar. Geol. 206, 19–40. doi:10.1016/j.margeo.2004.02.004

Cook, P.J., Shergold, J.H., 1984. Phosphorus, phosphorites and skeletal evolution at the Precambrian—Cambrian boundary. Nature 308, 231–236. doi:10.1038/308231a0

Cordell, D., Drangert, J.-O., White, S., 2009. The story of phosphorus: Global food security and food for thought. Glob. Environ. Change, Traditional Peoples and Climate Change 19, 292–305. doi:10.1016/j.gloenvcha.2008.10.009

Cosmidis, J., Benzerara, K., Gheerbrant, E., Estève, I., Bouya, B., Amaghzaz, M., 2013. Nanometer-scale characterization of exceptionally preserved bacterial fossils in Paleocene phosphorites from Ouled Abdoun (Morocco). Geobiology 11, 139–153. doi:10.1111/gbi.12022

Crosby, C.H., Bailey, J.V., 2012. The role of microbes in the formation of modern and ancient phosphatic mineral deposits. Front. Microbiol. 3. doi:10.3389/fmicb.2012.00241

Crosby, C.H., Bailey, J.V., Sharma, M., 2014. Fossil evidence of iron-oxidizing chemolithotrophy linked to phosphogenesis in the wake of the Great Oxidation Event. Geology 42, 1015–1018. doi:10.1130/G35922.1

de Beer, D., Sauter, E., Niemann, H., Kaul, N., Foucher, J.-P., Witte, U., Schlüter, M., Boetius, A., 2006. In situ fluxes and zonation of microbial activity in surface sediments of the Håkon Mosby Mud Volcano. Limnol. Oceanogr. 51, 1315–1331. doi:10.4319/lo.2006.51.3.1315

Delaney, M.L., 1998. Phosphorus accumulation in marine sediments and the oceanic phosphorus cycle. Glob. Biogeochem. Cycles 12, 563–572. doi:10.1029/98GB02263

Eckardt, F.D., Kuring, N., 2005. SeaWiFS identifies dust sources in the Namib Desert. Int. J. Remote Sens. 26, 4159–4167. doi:10.1080/01431160500113112

Edwards, C.T., Pufahl, P.K., Hiatt, E.E., Kyser, T.K., 2012. Paleoenvironmental and taphonomic controls on the occurrence of Paleoproterozoic microbial communities in the 1.88 Ga Ferriman Group, Labrador Trough, Canada. Precambrian Res. 212–213, 91–106. doi:10.1016/j.precamres.2012.04.020

Filippelli, G.M., 2011. Phosphate rock formation and marine phosphorus geochemistry: the deep time perspective. Chemosphere 84, 759–766. doi:10.1016/j.chemosphere.2011.02.019

Filippelli, G.M., Delaney, M.L., 1996. Phosphorus geochemistry of equatorial Pacific sediments. Geochim. Cosmochim. Acta 60, 1479–1495. doi:10.1016/0016-7037(96)00042-7

Föllmi, K.B., 1996. The phosphorus cycle, phosphogenesis and marine phosphate-rich deposits. Earth-Sci. Rev. 40, 55–124. doi:10.1016/0012-8252(95)00049-6

Froelich, P.N., Arthur, M.A., Burnett, W.C., Deakin, M., Hensley, V., Jahnke, R., Kaul, L., Kim, K.-H., Roe, K., Soutar, A., Vathakanon, C., 1988. The origin of marine phosphorite. The results of the R.V. Robert D. Conrad Cruise 23-06 to the Peru shelf Early diagenesis of organic matter in Peru continental margin sediments: Phosphorite precipitation. Mar. Geol. 80, 309–343. doi:10.1016/0025-3227(88)90095-3

Gächter, R., Meyer, J.S., Mares, A., 1988. Contribution of bacteria to release and fixation of phosphorus in lake sediments. Limnol. Oceanogr. 33, 1542–1558. doi:10.4319/lo.1988.33.6part2.1542

Garrison, R.E., Kastner, M., 1990. Phosphatic Sediments and Rocks Recovered from the Peru Margin during ODP Leg 112. Proc Sci. Rep. ODP Leg 112 Peru Cont. Margin 112. doi:10.2973/odp.proc.sr.112.145.1990

Garrison, R.E., Kastner, M., Kolodny, Y., 1987. Phosphorites and phosphatic rocks in the Monterey Formation and related Miocene units, coastal California. Cenozoic Basin Dev. Coast. Calif. Rubey 6, 348–381.

Girnth, A.-C., Grünke, S., Lichtschlag, A., Felden, J., Knittel, K., Wenzhöfer, F., de Beer, D., Boetius, A., 2011. A novel, mat-forming Thiomargarita population associated with a sulfidic fluid flow from a deep-sea mud volcano. Environ. Microbiol. 13, 495–505. doi:10.1111/j.1462-2920.2010.02353.x

Goldhammer, T., Brüchert, V., Ferdelman, T.G., Zabel, M., 2010. Microbial sequestration of phosphorus in anoxic upwelling sediments. Nat. Geosci. 3, 557–561. doi:10.1038/ngeo913

Hiatt, E.E., Pufahl, P.K., Edwards, C.T., 2015. Sedimentary phosphate and associated fossil bacteria in a Paleoproterozoic tidal flat in the 1.85Ga Michigamme Formation, Michigan, USA. Sediment. Geol. 319, 24–39. doi:10.1016/j.sedgeo.2015.01.006

Holmkvist, L., Arning, E.T., Küster-Heins, K., Vandieken, V., Peckmann, J., Zabel, M., Jørgensen, B.B., 2010. Phosphate geochemistry, mineralization processes, and Thioploca distribution in shelf sediments off central Chile. Mar. Geol. 277, 61–72. doi:10.1016/j.margeo.2010.08.011

Inthorn, M., Mohrholz, V., Zabel, M., 2006. Nepheloid layer distribution in the Benguela upwelling area offshore Namibia. Deep Sea Res. Part Oceanogr. Res. Pap. 53, 1423–1438. doi:10.1016/j.dsr.2006.06.004

Jahnke, R.A., Emerson, S.R., Roe, K.K., Burnett, W.C., 1983. The present day formation of apatite in Mexican continental margin sediments. Geochim. Cosmochim. Acta 47, 259–266. doi:10.1016/0016-7037(83)90138-2

Jarvis, I., Burnett, W., Nathan, Y., Almbaydin, F., Attia, A., Castro, L., Flicoteaux, R., Hilmy, M.E., Husain, V., Qutawnah, A., others, 1994. Phosphorite geochemistry-state-of-the-art and environmental concerns. Eclogae Geol. Helvetiae 87, 643–700.

Jochum, K.P., Weis, U., Stoll, B., Kuzmin, D., Yang, Q., Raczek, I., Jacob, D.E., Stracke, A., Birbaum, K., Frick, D.A., Günther, D., Enzweiler, J., 2011. Determination of Reference Values for NIST SRM 610–617 Glasses Following ISO Guidelines. Geostand. Geoanalytical Res. 35, 397–429. doi:10.1111/j.1751-908X.2011.00120.x

Jones, D.S., Flood, B.E., Bailey, J.V., 2016. Metatranscriptomic insights into polyphosphate metabolism in marine sediments. ISME J. 10, 1015–1019. doi:10.1038/ismej.2015.169

Joosu, L., Lepland, A., Kirsimäe, K., Romashkin, A.E., Roberts, N.M.W., Martin, A.P., Črne, A.E., 2015. The REE-composition and petrography of apatite in 2 Ga Zaonega Formation, Russia: The environmental setting for phosphogenesis. Chem. Geol. 395, 88–107. doi:10.1016/j.chemgeo.2014.11.013

Jørgensen, B.B., Gallardo, V.A., 1999. Thioploca spp.: filamentous sulfur bacteria with nitrate vacuoles. FEMS Microbiol. Ecol. 28, 301–313. doi:10.1111/j.1574-6941.1999.tb00585.x

Kalanetra, K.M., Joye, S.B., Sunseri, N.R., Nelson, D.C., 2005. Novel vacuolate sulfur bacteria from the Gulf of Mexico reproduce by reductive division in three dimensions. Environ. Microbiol. 7, 1451–1460. doi:10.1111/j.1462-2920.2005.00832.x

Kent, A.J.R., Ungerer, C.A. “Andy,” 2005. Production of barium and light rare earth element oxides during LA-ICP-MS microanalysis. J. Anal. At. Spectrom. 20, 1256–1262. doi:10.1039/B505734E

Kniep, R., Busch, S., 1996. Biomimetic Growth and Self-Assembly of Fluorapatite Aggregates by Diffusion into Denatured Collagen Matrices. Angew. Chem. Int. Ed. Engl. 35, 2624–2626. doi:10.1002/anie.199626241

Kniep, R., Simon, P., 2006. Fluorapatite-Gelatine-Nanocomposites: Self-Organized Morphogenesis, Real Structure and Relations to Natural Hard Materials, in: Naka, K. (Ed.), Biomineralization I, Topics in Current Chemistry. Springer Berlin Heidelberg, pp. 73–125.

Konhauser, K., Riding, R., 2012. Bacterial Biomineralization, in: Knoll, A.H., Canfield, D.E., Konhauser, K.O. (Eds.), Fundamentals of Geobiology. John Wiley & Sons, Ltd, pp. 105–130.

Krajewski, K.P., van Cappellen, P., Trichet, J., Kuhn, O., Lucas, J., Martin-Algarra, A., Prevot, L., Tewari, V.C., Gaspar, L., Knight, R.I., Lamboy, M., 1994. Biological Processes and Apatite Formation in Sedimentary Environments. Eclogae Geol. Helvetiae 87, 701–745.

Lamboy, M., 1994. Nannostructure and genesis of phosphorites from ODP Leg 112, the Peru margin. Mar. Geol. 118, 5–22. doi:10.1016/0025-3227(94)90110-4

Lamboy, M., 1993. Phosphatization of calcium carbonate in phosphorites: microstructure and importance. Sedimentology 40, 53–62. doi:10.1111/j.1365-3091.1993.tb01090.x

Lamboy, M., 1990a. Microstructures of a Phosphatic Crust from the Peruvian Continental-Margin - Phosphatised Bacteria and Associated Phenomena. Oceanol. Acta 13, 439–451.

Lamboy, M., 1990b. Microbial mediation in phosphatogenesis: new data from the Cretaceous phosphatic chalks of northern France. Geol. Soc. Lond. Spec. Publ. 52, 157–167. doi:10.1144/GSL.SP.1990.052.01.11

Lang, L., Kirsimäe, K., Vahur, S., 2016. Diagenetic fate of bioapatite in linguliform brachiopods: multiple apatite phases in shells of Cambrian lingulate brachiopod Ungula ingrica (Eichwald). Lethaia 49, 13–27. doi:10.1111/let.12127

Lécuyer, C., Reynard, B., Grandjean, P., 2004. Rare earth element evolution of Phanerozoic seawater recorded in biogenic apatites. Chem. Geol. 204, 63–102. doi:10.1016/j.chemgeo.2003.11.003

Lepland, A., Joosu, L., Kirsimäe, K., Prave, A.R., Romashkin, A.E., Črne, A.E., Martin, A.P., Fallick, A.E., Somelar, P., Üpraus, K., Mänd, K., Roberts, N.M.W., van Zuilen, M.A., Wirth, R., Schreiber, A., 2013a. Potential influence of sulphur bacteria on Palaeoproterozoic phosphogenesis. Nat. Geosci. 7, 20–24. doi:10.1038/NGEO2005

Lepland, A., Melezhik, V.A., Papineau, D., Romashkin, A.E., Joosu, L., 2013b. The Earliest Phosphorites: Radical Change in the Phosphorus Cycle During the Palaeoproterozoic, in: Melezhik, V.A., Prave, A.R., Hanski, E.J., Fallick, A.E., Lepland, A., Kump, L.R., Strauss, H. (Eds.), Reading the Archive of Earth's Oxygenation, Frontiers in Earth Sciences. Springer Berlin Heidelberg, pp. 1275–1296.

Lewy, Z., 1990. Pebbly phosphate and granular phosphorite (Late Cretaceous, southern Israel) and their bearing on phosphatization processes. Geol. Soc. Lond. Spec. Publ. 52, 169–178. doi:10.1144/GSL.SP.1990.052.01.12

Lin, K., Wu, C., Chang, J., 2014. Advances in synthesis of calcium phosphate crystals with controlled size and shape. Acta Biomater. 10, 4071–4102. doi:10.1016/j.actbio.2014.06.017

Liu, Y.-G., Miah, M.R.U., Schmitt, R.A., 1988. Cerium: A chemical tracer for paleo-oceanic redox conditions. Geochim. Cosmochim. Acta 52, 1361–1371. doi:10.1016/0016-7037(88)90207-4

Lyons, T.W., Reinhard, C.T., Planavsky, N.J., 2014. The rise of oxygen in Earth's early ocean and atmosphere. Nature 506, 307–15. doi:10.1038/nature13068

Martin, R.E., 1996. Secular increase in nutrient levels through the Phanerozoic; implications for productivity, biomass, and diversity of the marine biosphere. PALAIOS 11, 209–219. doi:10.2307/3515230

Meldrum, F.C., Cölfen, H., 2008. Controlling Mineral Morphologies and Structures in Biological and Synthetic Systems. Chem. Rev. 108, 4332–4432. doi:10.1021/cr8002856

Meldrum, F.C., Hyde, S.T., 2001. Morphological influence of magnesium and organic additives on the precipitation of calcite. J. Cryst. Growth 231, 544–558. doi:10.1016/S0022-0248(01)01519-6

Monteiro, P.M.S., van der Plas, A., Mohrholz, V., Mabille, E., Pascall, A., Joubert, W., 2006. Variability of natural hypoxia and methane in a coastal upwelling system: Oceanic physics or shelf biology? Geophys. Res. Lett. 33, L16614. doi:10.1029/2006GL026234

Mullins, H.T., Rasch, R.F., 1985. Sea-floor phosphorites along the Central California continental margin. Econ. Geol. 80, 696–715. doi:10.2113/gsecongeo.80.3.696

Murray, J., Renard, A.F., 1891. Report on the Deep Sea Deposits Based on Specimens Collected during the Voyage of the HMS, in: Challenger: Report on the Scientific Results of the Exploring Voyage of HMS Challenger 1873–1876. Her Majesty's Stationary Office, London, pp. 391–400.

O'Brien, G., Heggie, D., 1988. East Australian Continental Margin phosphorites. Eos Trans. Am. Geophys. Union 69, 2–2. doi:10.1029/88EO00007

O'Brien, G.W., Harris, J.R., Milnes, A.R., Veeh, H.H., 1981. Bacterial origin of East Australian continental margin phosphorites. Nature 294, 442–444. doi:10.1038/294442a0

O'Brien, G.W., Veeh, H.H., 1980. Holocene phosphorite on the East Australian continental margin. Nature 288, 690–692. doi:10.1038/288690a0

Omelon, S., Ariganello, M., Bonucci, E., Grynpas, M., Nanci, A., 2013. A review of phosphate mineral nucleation in biology and geobiology. Calcif. Tissue Int. 93, 382–96. doi:10.1007/s00223-013-9784-9

Papineau, D., 2010. Global biogeochemical changes at both ends of the Proterozoic: insights from phosphorites. Astrobiology 10, 165–181. doi:10.1089/ast.2009.0360

Papineau, D., Purohit, R., Fogel, M.L., Shields-Zhou, G.A., 2013. High phosphate availability as a possible cause for massive cyanobacterial production of oxygen in the Paleoproterozoic atmosphere. Earth Planet. Sci. Lett. 362, 225–236. doi:10.1016/j.epsl.2012.11.050

Planavsky, N.J., Rouxel, O.J., Bekker, A., Lalonde, S.V., Konhauser, K.O., Reinhard, C.T., Lyons, T.W., 2010. The evolution of the marine phosphate reservoir. Nature 467, 1088–1090. doi:10.1038/nature09485

Pufahl, P.K., Hiatt, E.E., 2012. Oxygenation of the Earth's atmosphere–ocean system: A review of physical and chemical sedimentologic responses. Mar. Pet. Geol. 32, 1–20. doi:10.1016/j.marpetgeo.2011.12.002

Qu, Y., Crne, A.E., Lepland, A., van Zuilen, M. a, 2012. Methanotrophy in a Paleoproterozoic oil field ecosystem, Zaonega Formation, Karelia, Russia. Geobiology 10, 467–78. doi:10.1111/gbi.12007

Rao, V.P., Nair, R.R., 1988. Microbial origin of the phosphorites of the western continental shelf of India. Mar. Geol. 84, 105–110. doi:10.1016/0025-3227(88)90128-4

Rao, V.P., Rao, K.M., Raju, D.S.N., 2000. Quaternary Phosphorites from the Continental Margin Off Chennai, Southeast India: Analogs of Ancient Phosphate Stromatolites. J. Sediment. Res. 70, 1197–1209. doi:10.1306/012400701197

Reimers, C.E., Ruttenberg, K.C., Canfield, D.E., Christiansen, M.B., Martin, J.B., 1996. Porewater pH and authigenic phases formed in the uppermost sediments of the Santa Barbara Basin. Geochim. Cosmochim. Acta 60, 4037–4057. doi:10.1016/S0016-7037(96)00231-1

Reynard, B., Lécuyer, C., Grandjean, P., 1999. Crystal-chemical controls on rare-earth element concentrations in fossil biogenic apatites and implications for paleoenvironmental reconstructions. Chem. Geol. 155, 233–241. doi:10.1016/S0009-2541(98)00169-7

Rogers, J., Bremner, J.M., 1991. The Benguela ecosystem. Part VII. Marine-geological aspects. Oceanogr. Mar. Biol. Annu. Rev. Vol 29 1–85.

Ruan, Q., Zhang, Y., Yang, X., Nutt, S., Moradian-Oldak, J., 2013. An amelogenin–chitosan matrix promotes assembly of an enamel-like layer with a dense interface. Acta Biomater. 9, 7289–7297. doi:10.1016/j.actbio.2013.04.004

Ruttenberg, K.C., 2014. The Global Phosphorus Cycle, in: Turekian, K.K. (Ed.), Treatise on Geochemistry: Second Edition. Elsevier, Oxford, pp. 499–558.

Ruttenberg, K.C., Berner, R.A., 1993. Authigenic apatite formation and burial in sediments from non-upwelling, continental margin environments. Geochim. Cosmochim. Acta 57, 991–1007. doi:10.1016/0016-7037(93)90035-U

Salman, V., Bailey, J.V., Teske, A., 2013. Phylogenetic and morphologic complexity of giant sulphur bacteria. Antonie Van Leeuwenhoek 104, 169–186. doi:10.1007/s10482-013-9952-y

Schenau, S.., Slomp, C.., De Lange, G.., 2000. Phosphogenesis and active phosphorite formation in sediments from the Arabian Sea oxygen minimum zone. Mar. Geol. 169, 1–20. doi:10.1016/S0025-3227(00)00083-9

Schuffert, J.D., Kastner, M., Jahnke, R.A., 1998. Carbon and phosphorus burial associated with modern phosphorite formation. Mar. Geol. 146, 21–31. doi:10.1016/S0025-3227(97)00122-9

Schulz, H.N., 1999. Dense Populations of a Giant Sulfur Bacterium in Namibian Shelf Sediments. Science 284, 493–495. doi:10.1126/science.284.5413.493

Schulz, H.N., Schulz, H.D., 2005. Large Sulfur Bacteria and the Formation of Phosphorite. Science 307, 416–418. doi:10.1126/science.1103096

Simon, P., Zahn, D., Lichte, H., Kniep, R., 2006. Intrinsic Electric Dipole Fields and the Induction of Hierarchical Form Developments in Fluorapatite–Gelatine Nanocomposites: A General Principle for Morphogenesis of Biominerals? Angew. Chem. Int. Ed. 45, 1911–1915. doi:10.1002/anie.200504465

Singer, E., Emerson, D., Webb, E.A., Barco, R.A., Kuenen, J.G., Nelson, W.C., Chan, C.S., Comolli, L.R., Ferriera, S., Johnson, J., Heidelberg, J.F., Edwards, K.J., 2011. Mariprofundus ferrooxydans PV-1 the First Genome of a Marine Fe(II) Oxidizing Zetaproteobacterium. PLOS ONE 6, e25386. doi:10.1371/journal.pone.0025386

Smith, E.A.H., Mayfield, C.I., Wong, P.T.S., 1977. Colonization and Decomposition of Fish Bone Material in Natural and Synthetic Aqueous Solutions. J. Fish. Res. Board Can. 34, 2164–2175. doi:10.1139/f77-285

Stille, P., Clauer, N., 1994. The process of glauconitization: chemical and isotopic evidence. Contrib. Mineral. Petrol. 117, 253–262. doi:10.1007/BF00310867

Summerhayes, C.P., Birch, G.F., Rogers, J., Dingle, R.V., 1973. Phosphate in Sediments off South-western Africa. Nature 243, 509–511. doi:10.1038/243509a0

Taylor, S.R., McLennan, S.M., 1985. The continental crust: Its composition and evolution. Blackwell Scientific Pub., Palo Alto, CA.

Tyrrell, T., 1999. The relative influences of nitrogen and phosphorus on oceanic primary production. Nature 400, 525–531. doi:10.1038/22941

Vallet-Regí, M., González-Calbet, J.M., 2004. Calcium phosphates as substitution of bone tissues. Prog. Solid State Chem. 32, 1–31. doi:10.1016/j.progsolidstchem.2004.07.001

van Cappellen, P., Berner, R.A., 1991. Fluorapatite crystal growth from modified seawater solutions. Geochim. Cosmochim. Acta 55, 1219–1234. doi:10.1016/0016-7037(91)90302-L

Veeh, H.H., Burnett, W.C., Soutar, A., 1973. Contemporary Phosphorites on the Continental Margin of Peru. Science 181, 844–845.

Veeh, H.H., Calvert, S.E., Price, N.B., 1974. Accumulation of uranium in sediments and phosphorites on the South West African shelf. Mar. Chem. 2, 189–202. doi:10.1016/0304-4203(74)90014-0

Wigley, R.A., Compton, J.S., 2006. Late Cenozoic evolution of the outer continental shelf at the head of the Cape Canyon, South Africa. Mar. Geol. 226, 1–23. doi:10.1016/j.margeo.2005.09.015

Wigley, R., Compton, J.S., 2007. Oligocene to Holocene glauconite–phosphorite grains from the Head of the Cape Canyon on the western margin of South Africa. Deep Sea Res. Part II Top. Stud. Oceanogr., Authigenic Mineral Formation in the Marine Environment; Pathways, Processes and Products 54, 1375–1395. doi:10.1016/j.dsr2.2007.04.004

Wu, Y.-J., Tseng, Y.-H., Chan, J.C.C., 2010. Morphology Control of Fluorapatite Crystallites by Citrate Ions. Cryst. Growth Des. 10, 4240–4242. doi:10.1021/cg100859m

Zanin, Y.N., Zamirailova, A.G., 2011. The history of the study of bacterial/cyanobacterial forms in phosphorites. Russ. Geol. Geophys., Problems of Regional Geology and Sedimentology (to the 100th birthday anniversary of Aleksandr Leonidovich Yanshin) 52, 1134–1139. doi:10.1016/j.rgg.2011.09.007

Lihtlitsents lõputöö reprodutseerimiseks ja lõputöö üldsusele kättesaadavaks tegemiseks

Mina, Kaarel Mänd ,

1. annan Tartu Ülikoolile tasuta loa (lihtlitsentsi) enda loodud teose

Geochemistry, microstructure and origin of recent phosphorites on the Namibian margin

mille juhendajad on Kalle Kirsimäe ja Aivo Lepland ,

1.1. reprodutseerimiseks säilitamise ja üldsusele kättesaadavaks tegemise eesmärgil, sealhulgas digitaalarhiivi DSpace-is lisamise eesmärgil kuni autoriõiguse kehtivuse tähtaja lõppemiseni;

1.2. üldsusele kättesaadavaks tegemiseks Tartu Ülikooli veebikeskkonna kaudu, sealhulgas digitaalarhiivi DSpace´i kaudu alates **20.05.2018** kuni autoriõiguse kehtivuse tähtaja lõppemiseni.

2. olen teadlik, et nimetatud õigused jäävad alles ka autorile.

3. kinnitan, et lihtlitsentsi andmisega ei rikuta teiste isikute intellektuaalomandi ega isikuandmete kaitse seadusest tulenevaid õigusi.

Tartus, **20.05.2016**